STEADY STATE SPECTRUM AND WAVE ENERGY OF PARAMETRIC DECAY INSTABILITY IN PLASMA

S. Y. Yuen

June 1979
M.I.T. Plasma Fusion Center Report RR-79-12

Steady state spectrum and wave energy of parametric decay instability in plasma

S. Y. Yuen

Francis Bitter National Magnet Laboratory,*
Massachusetts Institute of Technology, Cambridge, MA 02139

ABSTRACT

The nonlinear saturation of parametric decay instability in a plasma is investigated analytically under a wide range of conditions. Nonlinear coupling of four Langmuir waves is studied as a new saturation mechanism, which is treated together with three-wave cascade coupling and ion nonlinear Landau damping. It is found that when the electron and ion temperatures are almost equal, nonlinear four-wave coupling is the dominant saturation mechanism, which produces a single-peaked Langmuir wave spectrum. When the electron temperature far exceeds the ion temperature, cascade mode coupling is more important and the resulting spectrum exhibits many well-resolved peaks. All these features are in agreement with laboratory experiments.

I. INTRODUCTION

Under an intense high frequency electromagnetic field various modes of oscillation in a plasma may be coupled and driven unstable. The study of parametric instabilities so excited in a plasma has attracted much attention in the past few years because of their relevance to plasma heating.[1] Once above threshold the plasma wave amplitudes grow exponentially in time or space, and finally saturates due to nonlinear effects. The saturated plasma wave energy and spectrum are important quantities to know since they determine the rate of anomalous absorption.[2]

Various physical mechanisms for nonlinear saturation has been studied.[3] In the strong turbulence regime, when $|E_o|^2/4\pi nT_e \gtrsim 1$, computer simulations show particle trapping and wave saturation accompanied by turbulent heating of the plasma and formation of suprathermal electron tails[4,5] (E_o is the pump electric field, n the plasma density and T_e the electron temperature). At lower pump intensity, but $|E_o|^2/4\pi nT_e > \lambda_D k$, saturation by Langmuir wave collapse and soliton formation is predicted[6,7] (k is the wavevector of the Langmuir wave and λ_D the Debye wavelength).

In the weak turbulence regime, $|E_o|^2/4\pi nT_e < \lambda_D k$, the dominant saturating mechanism is considered to be multiple decay processes, i.e., ion nonlinear Landau damping if $T_e \simeq T_i$ when the ion acoustic wave is heavily damped,[8,9] and cascade mode coupling if $T_e \gg T_i$ when the ion wave is well defined.[10,11] The essential features predicted by these multiple-decay processes are a saturated Langmuir wave energy

P_ℓ proportional to the square of the pump intensity P_o, and a Langmuir wave spectrum consisting of a series of peaks separated from each other by the ion acoustic frequency.

In early experiments[12] the $P_\ell \propto P_o^2$ dependence can be directly inferred from absorption measurements near threshold. However, in more recent experiments[13-15] the $P_\ell \propto P_o^2$ relation is not observed. Mizuro and Degroot report that for $T_e/T_i \simeq 8$, $P_o \sim P_\ell$ from $P_o/P_{th} \gtrsim 1$ to $P_o/P_{th} \simeq 30$.[13] Flick's experimental data at $T_e \simeq T_i$ show that near threshold P_{th}, P_ℓ varies much faster than P_o^2, while for $P_o/P_{th} \gtrsim 3$, P_ℓ varies linearly as P_o.[14, 15]

For $T_e \gg T_i$, experimentally observed steady-state Langmuir wave spectra consist of discrete lines[16, 17] in agreement with cascade mode coupling theories.[10, 11] When $T_e \simeq T_i$, nonlinear ion Landau damping theories[8, 9] predict a similar spectrum. However, although the theoretically predicted spectrum is consistent with ionosphere measurements, it is not consistent with laboratory experiments.[14, 15] Instead, Flick reports an essentially single-peaked spectrum for P_o/P_{th} varying from 1 to 10. Since distinct peaks are fine structures and may not be experimentally resolved, it is important to note that while theories predict wave energy being spread into modes with much lower wavevector via secondary ion nonlinear Landau damping,[8, 9] such spread is not observed in Flick's experiments, which shows the wave energy to be concentrated around the original linearly excited frequency.[14, 15] Thus it seemed that where $T_e \simeq T_i$, nonlinear ion Landau damping alone cannot fully account for the nonlinear saturation of parametric decay instabilities.

In this article nonlinear coupling of four Langmuir waves is studied as an additional saturating mechanism,[18] which is treated together with the usual multiple-decay processes. The physical process of nonlinear four-wave coupling is as follows: a pump wave with electric field E_o and frequency $\omega_o \gtrsim \omega_{pe}$ excites Langmuir waves $E_\ell(\vec{k})$ and ion acoustic waves $E_a(\vec{k})$ through linear parametric decay instability. Two of the excited Langmuir waves then couple with each other to produce two new Langmuir waves with different wavevector $\vec{k}$. Note that nonlinear three-wave coupling between Langmuir waves cannot occur because frequency and wavevector conservation conditions cannot be satisfied. Nonlinear four-wave coupling spreads wave energy to modes with both higher and lower phase velocity, in contrast to the multiple-decay processes by which wave energy is spread to higher phase velocity modes only.

The importance of saturation by nonlinear four-wave coupling at $T_e \simeq T_i$ can be recognized if one recalls that the oscillating two stream instability (OTSI) is essentially a four-wave process with two of the waves involved being the pump, and it is well known that at $T_e \approx T_i$ the decay and OTSI have comparable thresholds.[19] Both the decay and OTSI are included in our general formulation, and the nonlinear four-wave saturating mechanism applies to both branches. However, the OTSI occupies a different region of k-space as the decay branch. When $T_e \approx T_i$, the volume of k-space occupied by OTSI is much smaller than that occupied by the decay unstable waves, and when $T_e \gg T_i$, the OTSI has much higher threshold than the decay instability. Therefore we present the saturated spectrum of the parametric decay

instability only, so that the physical features resulting from nonlinear saturation will not be obscured by mathematical complexities arising from a disjoint branch, and it is easier to compare with previous theoretical results where the OTSI branch is also neglected under the same conditions.[8-11]

Four-wave coupling processes can become strongly nonlinear, involving soliton formation and collapse.[20] We will not consider such processes and limit ourselves to the weak turbulence regime so that $|E_{\ell}(k)|^2/4\pi nT_e < \lambda_D k$. This condition is hard to satisfy for parametric instabilities in overdense or critically-dense plasmas, but can easily be satisfied in underdense plasmas. Since we are interested in the decay branch of parametric instabilities, we will always consider the pump frequency ω_o to be greater than the electron plasma frequency ω_{pe}.

The present theory is valid over a wide range of temperature ratios, and the damping rate of the ion acoustic wave, γ_a/ω_a, is used as a continuously varying parameter. It is found that when $\gamma_a/\omega_a \ll 1$ ($T_e \gg T_i$), nonlinear four-wave coupling and ion nonlinear Landau damping are neglible compared to cascade mode coupling, and the previously predicted[10,11] comb-like Langmuir wave spectrum is obtained. As γ_a/ω_a increases, nonlinear four-wave coupling and ion nonlinear Landau damping become more and more important, the number of separate peaks in the saturated spectrum decreases and the peaks broadens. When the ion acoustic wave is heavily damped ($\gamma_a/\omega_a \simeq 1$, $T_e \simeq T_i$), nonlinear four-wave coupling becomes the dominant saturating mechanism, and the saturated Langmuir wave

spectrum obtained in this case consist of a single broad peak with wave energy concentrating around the linearly excited frequency. All these results are in agreement with laboratory experimental observations.[14-17] Our theory also predicts a saturated Langmuir wave energy which increases very fast with P_o when $P_o \gtrsim P_{th}$, but linearly proportional to P_o when $P_o/P_{th} \gtrsim 3$, again in agreement with experiments.[13-15]

At $T_e \simeq T_i$, the present theory yields results quite different from the ion nonlinear Landau damping theories.[8,9] It should be noted that the ion nonlinear Landau damping theories predict Langmuir wave energy being cascaded into modes with very small wavevector. Under such situation strongly turbulent Langmuir wave collapse can easily set in,[20] leading to the total breakdown of the weak turbulence theory. However, the present theory does not predict any cascading for this temperature condition, so that the weak turbulence condition can be satisfied. For $T_e \gg T_i$, when cascading does occur, the four-wave process which leads to Langmuir wave collapse is very weak.[20]

The coupled mode equations governing the evolution of the Langmuir and ion acoustic waves are derived in the next section. Section III briefly checks the present formulation with previous theories by calculating the linear growth rate and threshold. In Sec. IV a steady-state solution to the coupled-mode equations are obtained by using various approximations, yielding the saturated Langmuir wave spectrum in the one-dimensional case. The total steady-state Langmuir wave energy is calculated in Sec. V. In Sec. VI the major approximations used in the calculation are summarized and their effects and range of validity discussed. The stability of the steady-state solution is also examined.

II. COUPLED-MODE EQUATIONS

Consider a homogeneous, warm plasma without any external magnetic field. All collective oscillations of the plasma can be represented by the total spatial-temporal dependent electric field $\vec{\mathcal{E}}(\vec{r}, t)$ governed by the wave equation

$$\vec{\nabla} \times (\vec{\nabla} \times \vec{\mathcal{E}}) + \frac{1}{c^2} \frac{\partial^2 \vec{\mathcal{E}}}{\partial t^2} = - \frac{4\pi}{c^2} \frac{\partial^2 \vec{\mathcal{P}}}{\partial t^2} \tag{1}$$

where $\vec{\mathcal{P}}$ is the total polarization of the plasma. We work in the electrostatic approximation so that

$$\vec{\nabla} \cdot \vec{\mathcal{P}} = - \rho = - \sum_a n_a q_a \int f_a (\vec{r}, \vec{v}, t) d\vec{v} \tag{2}$$

where ρ is the average charge density, q_a and n_a are the charge and equilibrium density of the a species particle (a = e, i for electron and ion), and $f_a(\vec{r}, \vec{v}, t)$ is the particle distribution function governed by the Vlasov equation

$$\frac{\partial f_a}{\partial t} + \vec{v} \cdot \frac{\partial f_a}{\partial \vec{r}} + \frac{q_a}{m_a} \vec{\mathcal{E}}(\vec{r}, t) \cdot \frac{\partial f_a}{\partial \vec{v}} = 0. \tag{3}$$

Equations (1) - (3) are the basis of our analysis. To proceed with the case of parametric instabilities, we expand $\vec{\mathcal{E}}(\vec{r}, t)$ in terms of three groups of modes: a monochromatic pump $\vec{E}_o$, the high frequency Langmuir waves $\vec{E}_\ell(\vec{k})$, and the low frequency ion acoustic modes $\vec{E}_a(\vec{k})$,

$$\vec{\mathcal{E}}(r,t) = \vec{E}_o e^{i(k_o z - \omega_o t)} + \int d\vec{k}\, \vec{E}_\ell(\vec{k}) e^{i(\vec{k}\cdot\vec{r} - \omega_{\ell\vec{k}} t)} + \int d\vec{k}\, \vec{E}_a(\vec{k}) e^{i(\vec{k}\cdot\vec{r} - \omega_{a\vec{k}} t)} \quad (4)$$

where $\vec{E}_\ell(\vec{k})$ and $\vec{E}_a(\vec{k})$ depend on time only, and $\vec{k} \times \vec{E}_\ell(\vec{k}) = \vec{k} \times \vec{E}_a(\vec{k}) = 0$. Nonlinearity of the pump field is neglected so that $\vec{E}_o$ is a constant. However, it must be noted that the nonlinear interaction between the pump and decay waves is a saturation mechanism intrinsic to all parametric processes. This effect has been studied previously.[21, 11] Because of mode coupling, the oscillating frequencies $\omega_{\ell\vec{k}}$ and $\omega_{a\vec{k}}$ of $\vec{E}_\ell(\vec{k})$ and $\vec{E}_a(\vec{k})$ need not satisfy the Bohn-Gross dispersion relations $\bar{\omega}_{\ell\vec{k}} = \omega_{pe}(1 + 3k^2)^{1/2}$, $\bar{\omega}_{a\vec{k}} = \omega_{pi}\left[3k^2/(1 + 3k^2)\right]^{1/2}$. All wavevectors are normalized with respect to the Debye wavevector. With expansion Eq. (4) the wave equation can be written as

$$\left\{ \frac{1}{\omega_{\ell k}^2} \frac{\partial^2}{\partial t^2} - \frac{2i}{\omega_{\ell k}} \frac{\partial}{\partial t} - 1 \right\} \vec{E}_\ell(\vec{k}) = 4\pi \vec{\mathcal{P}}(\vec{k}, \omega_{\ell k}) \quad (5)$$

$$\left\{ \frac{1}{\omega_{ak}^2} \frac{\partial^2}{\partial t^2} - \frac{2i}{\omega_{ak}} \frac{\partial}{\partial t} - 1 \right\} \vec{E}_a(\vec{k}) = 4\pi \vec{\mathcal{P}}(\vec{k}, \omega_{ak}) \quad (6)$$

To find the plasma polarization, we use the standard iterative scheme to solve Eqs. (2) and (3). Writing Eqs. (2) and (3) in their Fourier transform form, we let

$$f_a(\vec{v}, \vec{k}, \omega) = f_{ao}(\vec{v})\delta(\vec{k})\delta(\omega) + f_{a1} + f_{a2} + f_{a3} + \ldots \quad (7)$$

$$\rho(\vec{k}, \omega) = \rho_1(\vec{k}, \omega) + \rho_2(\vec{k}, \omega) + \rho_3(\vec{k}, \omega) + \ldots \quad (8)$$

where the equilibrium distribution $f_{\alpha o}(\vec{v})$ is Maxwellian, and

$$f_{\alpha n}(\vec{v},\vec{k},\omega) = -i\,\frac{q_\alpha}{m_\alpha}\int d\vec{k}'\,d\omega'\,\frac{1}{\omega-\vec{k}\cdot\vec{v}}\,\vec{\mathcal{E}}(\vec{k}-\vec{k}',\omega-\omega')\cdot\nabla_v f_{\alpha n-1}(\vec{v},\vec{k}',\omega') \tag{9}$$

The equilibrium electron density is exactly cancelled by the positive ions, so that $\rho_o = 0$.

From Eqs. (7) and (9) we see that $f_{\alpha 1}$ is proportional to $\mathcal{E}$, and describes the linear response of the plasma system. The term $f_{\alpha 2}$ goes as $\mathcal{E}^2$ and takes into account three-wave coupling processes, which include the linear parametric excitation of Langmuir and ion waves by the pump (see Fig. 1a), and the nonlinear coupling between two Langmuir waves and an ion acoustic wave, i.e., cascade mode coupling (Figs. 1c, 1d). The term $f_{\alpha 3}$ is proportional to $\mathcal{E}^3$ and takes into account four-wave coupling processes, which includes the linear excitation of two Langmuirs by two pump waves simultaneously, i.e., OTSI, (Fig. 1b) and the nonlinear coupling between four Lagnmuir waves (Fig. 1e). In the problem we are considering, these are all the mode coupling processes that can satisfy the frequency-wavevector conservation conditions, and are depicted schematically in Fig. 1.

Note that in Eq. (9) the electric field $\mathcal{E}$ is always an first-order quantity, we are not expanding it in perturbative terms as we did with f_α and ρ. Therefore only coupling between collective modes are included in the derivation. The wave-particle nonlinear interaction, i.e., the nonlinear ion Landau damping term as depicted in Fig. 1f, is derived separately[22] and included as an additional loss term in the wave equation.

From Eqs. (2) and (7)-(9), the plasma polarization can be written as

$$4\pi\epsilon^{L}(\vec{k},\omega)\mathcal{P}(\vec{k},\omega) = [\rho_2(\vec{k},\omega) + \rho_3(\vec{k},\omega)]/(-i|k|)$$

$$= \int d\vec{k}'\, d\omega'\, \tilde{\chi}^{(2)}(\vec{k},\omega;\vec{k}',\omega')\vec{\mathcal{E}}(\vec{k}',\omega')\vec{\mathcal{E}}(\vec{k}-\vec{k}',\omega-\omega') \qquad (10)$$

$$+ \int d\vec{k}'\, d\vec{k}''\, d\omega'\, d\omega''\ \tilde{\chi}^{(3)}(\vec{k},\omega,\vec{k}',\omega',\vec{k}'',\omega'')\vec{\mathcal{E}}(\vec{k}',\omega')\vec{\mathcal{E}}(\vec{k}'',\omega'')\vec{\mathcal{E}}(\vec{k}-\vec{k}'-\vec{k}'',\omega-\omega'-\omega'')$$

where $\epsilon^{L}(\vec{k},\omega)$ is the longitudinal dielectric constant, derived from the f_{a1} term and include both electron and ion contributions. The ions are too heavy to follow the high frequency oscillation, thus do not contribute to the high frequency terms, but we have to keep the ion terms in the low frequency case. Also, the ions do not participate in the nonlinear coupling processes,[22] so that $\tilde{\chi}^{(2)}$ and $\tilde{\chi}^{(3)}$ are mainly from electron contribution. The first order nonlinear susceptibility $\tilde{\chi}^{(2)}$ has been calculated by many authors before.[22,23]

$$\tilde{\chi}^{(2)}(\vec{k},\omega;\vec{k}',\omega') \simeq -i\,(ek_D/2m_e\omega_o^2|k|)(\vec{k}\cdot\vec{k}'/|k||k'|) \qquad (11)$$

for coupling between longitudinal waves. The second-order nonlinear susceptibility $\tilde{\chi}^{(3)}$ can be obtained by simply carrying out the iteration in Eq. (9) for one more order,

$$\tilde{\chi}^{(3)}(\vec{k},\omega;\vec{k}',\omega',\vec{k}'',\omega'') = -2\left(\frac{ek_D}{2m_e\omega_o^2}\right)^2 \frac{(\vec{k}\cdot\vec{k}')\vec{k}''\cdot(\vec{k}-\vec{k}'-\vec{k}'')}{|k||k'||k''||k-k'-k''|} \qquad (12)$$

With Eqs. (10)-(12) we can write down the high and low frequency plasma polarizations. For simplicity we shall restrict to the one-dimensional case from now on. Writing out the specific modes included in Eq. (4), and

keeping only those processes that can satisfy frequency-wavevector matching conditions, we get

$$4\pi\epsilon^{L}(k,\omega_{\ell k})\mathcal{P}(k,\omega_{\ell k}) = -i(2\Lambda/k)\left\{E_o E_a^{*}(k) - \int dk'[\,E_\ell(k')E_a(k+k') - E_\ell(k')E_a^{*}(k+k')]\right\}$$

$$-8\Lambda^2\left\{E_o^{2}E_\ell^{*}(k) + \int dk dk' E_\ell^{*}(k')E_\ell(k'')E_\ell(k+k'-k'')\right\} \quad (13)$$

$$4\pi\epsilon^{L}(k,-\omega_{ak})\mathcal{P}(k,-\omega_{ak}) = -i(2\Lambda/k)\left\{E_o^{*}E_\ell(k) + \int dk' E_\ell(k')E_\ell^{*}(k-k')\right\} \quad (14)$$

where $\Lambda \equiv (64n\pi T_e)^{-1/2}$, and we have let $k_o = 0$, $E(-\omega) = E^{*}(\omega)$. The five terms on the right-hand side of Eq. (13) correspond to the process depicted in Figs. 1a, 1d, 1c, 1b and 1e, respectively. Only processes 1a, 1c and 1d are involved in the low frequency Eq. (14).

Although $E_\ell(k)$ and $E_a(k)$ may oscillate at any frequency, it is clear that they will peak around the natural resonance frequencies $\bar{\omega}_{\ell k}$ and $\bar{\omega}_{ak}$. Thus, we can expand $1/\epsilon^{L}(k,\omega)$ around the natural frequencies for each of the coupled mode terms. Take, for example, the first term on the right-hand side of Eq. (13), the $E_o E_a^{*}(k)$ term. Consider $E_a^{*}(k)$ to be at resonance, so that the frequency matching condition is $\omega_{\ell k} + \bar{\omega}_{ak} - \omega_o = 0$. However, we require that $\omega_{\ell k}$ to be near resonance $\bar{\omega}_{\ell k}$ also, so we can write for this term

$$\frac{1}{\epsilon^{L}(k,\omega_{\ell k})} \simeq -i\,\frac{\bar{\omega}_{\ell k}}{2\gamma_\ell}\,\frac{\gamma_\ell^{2}}{(\bar{\omega}_{\ell k}+\bar{\omega}_{ak}-\omega_o)^{2}+\gamma_\ell^{2}}$$

$$\simeq -i(\omega_{\ell k}/2\gamma_\ell)\, f\,[(k-k_d)/\sigma\Delta] \quad (15)$$

where γ_ℓ is the damping rate of the Langmuir wave, $\sigma \equiv \gamma_\ell/\omega_a$, $\Delta \equiv 2(m_e/3m_i)^{1/2}$, $k_d \equiv -\Delta/2 + (\Delta^2/4 + 2\epsilon/3)^{1/2}$, $\epsilon \equiv \omega_o/\omega_{pe} - 1$, and $f(x) \equiv 1/(1+x^2)$ for any x. Similar expansions can be readily carried for each of the seven terms on the right-hand side of Eqs. (13) and (14). The Lorentzian functions f(x) take into account frequency pulling effects so that coupling to modes with frequency shifted from the resonance frequency is allowed.

With Eq. (15) and similar expansions, we substitute the plasma polarization Eqs. (13) and (14) into Eqs. (5) and (6) and obtain the one-dimensional coupled-mode equation for Langmuir and ion acoustic waves:

$$(1/\omega_{\ell k})(\partial/\partial t + \gamma_\ell + \gamma_{NL})E_\ell(k) = -i(\Lambda/k)E_o E_a^*(k) - 4\Lambda^2 f_p E_o^2 E_\ell^*(k) + P_{NLS} \tag{16}$$

$$(1/\omega_{ak})(\partial/\partial t + \gamma_a)E_a(k) = -ik\Lambda f_d E_o E_\ell^*(k) + P'_{NLS} \tag{17}$$

where $f_p \equiv f[(k-k_p)/\sigma\Delta]$, $f_d \equiv f[(k-k_d)/\beta\Delta]$, $\beta \equiv \gamma_a/\omega_a$, $k_p \equiv (2\epsilon/3)^{1/2}$. Here we consider ω_o to be close to ω_p, so that only long wavelength collision damped waves are excited and the damping rates are independent of k. Also, we assume the electric field amplitudes to be slowly varying, so that the linearly growth rate is smaller than the real frequencies, thus the second order time derivative is neglected. Note that the Langmuir waves are generally lightly damped in the wavelength range of interest, $\gamma_\ell/\omega_a \ll 1$, thus in the three-wave coupling most of the frequency pulling effects comes from ion contribution, and anti-Stokes three-wave coupling can be neglected. The first two terms on the right-hand side of Eq. (16) account for linear decay and OTSI. The nonlinear mode coupling terms are:

$$P_{NLS} = i(\Lambda/k) \int dk' [E_\ell(k')\, E_a(k+k') - E_\ell(k)\, E_a^*(k+k')]$$

$$- 4\Lambda^2 \int dk'dk''\, f[(k-k')/\sigma\Delta]\, E_\ell^*(k') E_\ell(k'') E_\ell(k+k'-k'') \qquad (18)$$

$$P'_{NLS} = - ik\Lambda \int dk'\, f[(2k'-k-\Delta)/\beta\Delta]\, E_\ell(k') E_\ell^*(k'-k) \qquad (19)$$

The ion nonlinear damping term γ_{NL} in Eq. (16) is derived by previous authors,[22,8] and included in the coupled-mode equations as an additional loss term

$$\gamma_{NL} \simeq \Lambda^2 \int dk' \, |E_\ell(k')|^2 \left\{ f[(k-k'+\Delta)/\beta\Delta] - f[(k-k'-\Delta)/\beta\Delta] \right\} \qquad (20)$$

where we have approximated the plasma dispersion function by the function f. This should be a fairly good approximation as can be seen from Fig. 2, where the solid lines plots the tabulated[24] value of $M(\zeta) = (1/k^2)\mathrm{Im}[\epsilon^L(k-k', \bar{\omega}_{\ell k} - \bar{\omega}_{\ell' k'})]^{-1}$. In one dimension case, $\zeta \equiv (\bar{\omega}_{\ell k} - \bar{\omega}_{\ell' k'})/ v_{Ti} |k-k'| = (3T_e/2T_i)^{1/2}$ $[(|k| - |k'|)/\Delta]$, $v_{Ti} = (2T_i/m_i)^{1/2}$. The width of $M[(k-k')/\Delta]$ decreases with increasing T_e/T_i, this is approximated in Eq. (20) by the width decreases with decreasing γ_a/ω_a. The dashed line in Fig. 2 shows the approximated matrix element, which matches $M[(k-k')/\Delta]$ fairly closely except at the tail part. The approximation may be improved if we let f(x) to be a Gaussian instead of Lorentzian function of x as can be seen from the crosses in Fig. 2. We will let $f(x) = \exp(-x^2)$ from now on.

Equations (16) - (20) form the basis of subsequent analysis.

III. LINEAR GROWTH FUNCTION

Before we start to solve the nonlinear problem, let us quickly check the formulation by examining the linear growth behavior. Putting $\partial E(k)/\partial t = \gamma(k)E(k)$ and $P_{NLS} = P'_{NLS} = \gamma_{NL} = 0$, in Eqs. (16) and (17), the resulting secular equation has two doubly degenerate roots for the linear growth rate as a function of k

$$\gamma(k) = \frac{1}{2}\left\{-(\gamma_\ell+\gamma_a)+\omega_p f_p P_o \pm [(\gamma_\ell - \gamma_a - \omega_p f_p P_o)^2 + 4\omega_{\ell k}\omega_{ak} f_d P_o]^{1/2}\right\} \quad (21)$$

where $P_o \equiv |E_o|^2/64\pi n T_e$. With $\gamma(k) = 0$, Eq. (21) yields the threshold value for various region in k-space

$$\tilde{P}_{th}(k) = \gamma_\ell \gamma_a/(\omega_{\ell k}\omega_{ak} f_d + \gamma_a \omega_p f_p). \quad (22)$$

From Eq. (22) the minimum threshold for decay instability is $P_{th} = \gamma_\ell \gamma_a/\omega_{\ell k}\omega_{ak}$ occurring at $k = k_d$, miminum threshold for OTSI is $P_{om} = \gamma_\ell/\omega_p$. Equation (21) shows that the linear growth rate for the decay branch varies as $P_o^{1/2}$, while it varies as P_o for the OTSI branch. All these are in agreement with previous theories.[19]

The linear growth rate as a function of k has been computed numerically before,[4] but Eq. (21) allows us to tell at a glance what region of k space will be excited for an arbitrary set of parameters. For example, Fig. 3 plots Eq. (21) for a hydrogen plasma, it exhibits two distinct peaks for the decay and OTSI branches, with their relative height determined by P_o. The widths of the two peaks varies with the damping rate of the ion acoustic and Langmuir waves respectively, which is intuitively correct because the damping rates determines the range of k-space to be close to resonance.

IV. SATURATED SPECTRUM

As can be seen from Eq. (21) and Fig. 3, the OTSI occupies a different region of k-space as the decay branch. For $T_e \simeq T_i$ when OTSI has comparable threshold with the decay instability, $\gamma_\ell/\omega_a << 1$ implies the waves excited by OTSI concentrate in a very narrow region of k-space. Thus for simplicity we shall henceforth neglect the OTSI branch in our saturated spectrum and wave energy, although the saturation processes considered applies equally to both branches and it is straight forward to generalize the present calculation to cover OTSI as well.

In the steady state, $\partial E_\ell(k)/\partial t = \partial E_a(k)/\partial t = 0$, elminating $E_a(k)$ between Eqs. (16) and (17) gives

$$(\gamma_\ell + \gamma_{NL})E_\ell(k) = (\omega_\ell \omega_a/\gamma_a)\Lambda^2 f_d |E_o|^2 E_\ell(k)$$

$$- 4\omega_\ell\Lambda^2\int dk'dk'' f[(k-k')/\sigma\Delta] E_\ell^*(k') E_\ell(k'') E_\ell(k+k'-k'')$$

$$+ (\omega_\ell\omega_a/\gamma_a)\Lambda^2 \int dk'dk''\left\{f[(2k''-k-k'-\Delta)/\beta\Delta] - f[(2k''-k-k'+\Delta)/\beta\Delta]\right\} \cdot$$

$$\cdot E_\ell(k')E_\ell^*(k'')E_\ell(k+k'k''), \qquad (23)$$

where the $4\Lambda^2 f_p E_o^2 E_\ell^*(k)$ term in Eq. (16) representing OTSI is neglected, so are terms of order $f(k_d/\Delta)$ as compared to unity. The solution of Eq. (23) depends heavily on phase behavior. The following calculation will be carried out in the random phase approximation.

$$<E_\ell(k)E_\ell^*(k')> = <E_\ell(k)E_\ell(-k')> = |E_\ell(k)|^2 \delta(k-k'). \qquad (24)$$

When the pump wave is coherent, the random phase approximation may be justified by virtue of the many modes linearly excited. It must be noted that Eq. (24) can be used only within the weak turbulence regime we are

working with. When $P_o > \lambda_D k$, strongly nonlinear processes such as soliton formation sets in and the problem must be solved with coherent phase. Multiply Eq. (23) by $E^*(k''')$ and use Eq. (24), we get

$$f_d P_o - P_{th} = (1+\beta)\int dk' I(k')\left\{f[(k'-k+\Delta)/\beta\Delta] - f[(k'-k-\Delta)/\beta\Delta]\right\} + 4\beta\int dk' I(k') f[(k'-k)/\sigma\Delta] \qquad (25)$$

where $I(k) \equiv |E_\ell(k)|^2/64\pi n T_e$. The second term on the right-hand side represents nonlinear four-wave coupling, the part of the first term proportional to β comes from ion nonlinear Landau damping, and the rest of the second term is due to three-wave cascade mode coupling.

In the form Eq. (25), ion nonlinear Landau damping, three-wave and four-wave couplings all appear as the same order, the only difference between them being the coupling functions. Since the maximum value of f is always 1, the relative strength of various nonlinear processes can be seen at once from the coupling parameters. Thus when $\beta = 1$ four-wave coupling is more important, and when $\beta \ll 1$ three-wave cascading dominates.

The ordering of three- and four-wave processes in Eq. (25) may seem puzzling at first because four-wave coupling is apparently a higher order process than three-wave coupling as can be seen from Eq. (10). It must be remembered that one of the waves in three-wave processes is the acoustic wave $E_a(k)$, and when eliminating $E_a(k)$ the ordering changes. When $\gamma_a \omega_a \simeq 1$, the acoustic wave is so heavily damped that it can be adiabatically eliminated as a dynamical variable, in so doing $E_a(k)$ is treated as a second-order variable,[22] different from $E_\ell(k)$ which are first-order variables.

When $\gamma_a/\omega_a \ll 1$, $E_a(k)$ can be eliminated only in the steady state, is so doing we are essentially looking at a two-step three-wave process: a Langmuir wave decays into another Langmuir and an acoustic wave, which at once combine with a third Langmuir wave to produce a fourth one. Thus in an equation involving $E_\ell(k)$ only, all three processes appear as same order.

The exact solution of the integral Eq. (25) is sensitive to the specific functional form of the f's, including the tail behavior. Since approximation has already been made on the form of f, we do not seek exact numerical solutions to Eq. (25) but rather develop approximate analytic solutions.

If we drop the second term on the right-hand side, then Eq. (25) reduces to the case of cascade decay process. Kruer and Valeo[8] have solved such a problem numerically using the exact functional form of $M(\zeta)$. Their Langmuir spectrum shows a series of sharp spikes separated by Δ from each other. Physically, this is obvious because in the three-mode decay process, the two Langmuir modes have to be separated by the ion mode frequency. In fact, if we go to the extreme case and approximate all f's by delta functions, e.g., $f(k'-k\pm\Delta) \simeq \delta(k'-k\pm\Delta)$, then Eq. (25) can be solved exactly[11] and gives I(k) as a set of zero width lines with varying height locating at $k_n = k_d - n\Delta$.

The finite width of f will broaden these lines. Furthermore, the four-wave parametric process is not restricted by the wave numbers of the ion modes, so that its effect is to wash out the sharp spikes caused by the three-mode decay process. However, for any given $E_\ell(k)$, the range of wave number it can couple to via four-wave processes is of the order $\sigma\Delta$, so that in any one coupling process wave energy cannot spread to very different k-modes and alter the spectrum drastically.

With the above consideration, we assume the solution for I(k) to be consisting of a series of Gaussian functions g_n with varying normalizing height I_n and width $a_n\Delta$

$$I(k) = \sum_n I_n \exp[-(k-k_n)^2/(a_n\Delta)^2] - \Gamma \tag{26}$$

where I_n, a_n, Γ are unknown constants to be determined.

Substituting Eq. (26) into Eq. (25), we see that P_{th} and Γ are the only two terms independent of k. Since Eq. (25) has to be satisfied for all k values, Γ can be determined

$$\Gamma = P_{th}/4\sqrt{\pi}\,\beta\Delta \tag{27}$$

The physical meaning of Γ should be clear. All nonlinear processes considered here are just various parametric instabilities with the linearly excited Langmuir waves acting as pumps, and it is well known that parametric instabilities can occur only above a threshold. The constant Γ then serves as a threshold term which determines what k-modes are excited by linear as well as nonlinear processes.

With Eq. (26) the integration over k' in Eq. (25) can be carried out

$$f_d\tilde{P}_o = \sum_n A_n\left\{f[(k-k_{n-1})/w_{\beta n}] - f[(k-k_{n+1})/w_{\beta n}] + \sigma_n f[(k-k_n)/w_{\sigma n}]\right\} \tag{28}$$

where $\tilde{P}_o \equiv P_o/[(1+\beta)\beta\sqrt{\pi}\,\Delta]$, $w_{\beta n} \equiv (a_n^2+\beta^2)^{1/2}\Delta$; $w_{\sigma n} = (a_n^2+\sigma^2)^{1/2}\Delta$, $A_n \equiv a_n I_n (a_n^2+\beta^2)^{-1/2}$, $\sigma_n = 4\sigma w_{\beta n}/w_{\sigma n}(1+\beta)$. Note that the k_n's are separated from each other by Δ, and the width of the coupling functions are at most Δ when $\gamma_a/\omega_a = 1$. Thus we will assume that the line centering at $k = k_n$ couples to lines at $k = k_{n\pm1}$ only. This a good approximation as

long as the widths of individual lines in the spectrum are less than Δ ($a_n \lesssim 1$). Under this approximation Eq. (28) can be separated into a set of equations:

$$f_d \tilde{P}_o = A_1 f[(k-k_o)/w_{\beta 1}] + A_o \sigma_o f[(k-k_o)/w_{\sigma o}] \tag{29}$$

$$0 = A_{n+1} f[(k-k_n)/w_{\beta n+1}] + A_n \sigma_n f[(k-k_n)/w_{\sigma n}] \tag{30}$$

$$- A_{n-1} f[(k-k_n)/w_{\beta n-1}], \qquad n > 1$$

Only positive I_n's are included in Eq. (26), so that if I_{N+1} becomes negative, the series stops at I_N. In general, the I's increases with P_o, so that Eq. (26) shows the number of peaks N will also increase with P_o. This is physically obvious because a stronger pump just means more waves can be nonlinearly excited by secondary parametric processes, and agrees with experimental observations. When secondary decay peaks do appear, they only appear as P_o is raised further above threshold for the fundamental decay.[16,17] It is noted that experimentally when P_o is further increased, the distinct peaks broadens and finally smears out. This is probably due to thermal effects when the plasma is heated up, and is not considered in the present theory.

Since we are not concerned with the detailed shape of each peak, but are interested only in their heights and widths, we expand the f's in a Taylor series around k_n, and match the coefficients of the first two non-vanishing terms to calculate a_n and I_n. Equations (29) and (30) then gives

$$\tilde{P}_o = A_1 + \sigma_o A_o \tag{31}$$

$$0 = A_{n+1} + \sigma_n A_n - A_{n-1}, \qquad n \geq 1 \tag{32}$$

from the constant terms, and

$$\tilde{P}_o = \beta^2 (A'_1 + \sigma'_o A'_o) \tag{33}$$

$$0 = A'_{n+1} + \sigma'_n A'_n - A'_{n-1} \qquad - \qquad n \geq 1 \tag{34}$$

from the $(k-k_n)^2$ terms. Here $A'_n = a_n I_n (a_n^2 + \beta^2)^{-3/2}$, and $\sigma'_n = 4\sigma(1+\beta)^{-1}$ $[(a_n^2 + \beta^2)/(a_n^2 + \sigma^2)]^{-3/2}$

Equation (32) forms a set of linear transformations which can be represented in terms of continued fractions:[25]

$$A_n = A_{n+1} \left\{ \sigma_{n+1} + \cfrac{1}{\sigma_{n+2} + \cfrac{1}{\sigma_{n+3} + \cdots}} \right\} \tag{35}$$

then Eq. (31) becomes

$$\tilde{P}_o = A_o C \tag{36}$$

where C is a continued fraction

$$C = \sigma_o + \cfrac{1}{\sigma_1 + \cfrac{1}{\sigma_2 + \cdots}} \tag{37}$$

Similarly, we get for Eq. (33)

$$\tilde{P}_o/\beta^2 = A'_o C' \tag{38}$$

where C' is same as C with σ_n replaced by σ'_n. If we know C and C', Eqs. (36) and (38) can be solved for a_o, I_o, and it is straight forward to obtain all a_n and I_n's from Eqs. (31) - (34). However, C and C' themselves depend on the a_n's. We will use an interative scheme to obtain approximate solutions.

In the zeroth approximation, we assume all a_n's are equal, and let $a_n^o = \beta$ in Eq. (37). We then solve for all the a_n' and I_n''s. The first order values a_n' are then substituted back into Eq. (37) to calculate C in the first-order approximation. This iterative procedure may be continued. It is found that the values of a_n obtained settles quickly after the first iteration. In general, the result of the second and seventh iteration will not differ by more than five percent. The choice $a_n^o = \beta$ comes from the consideration that spectral lines broadens with increasing ion acoustic damping. As it turns out, the final results of a_n are quite insensitive to small variation to the values of a_n' used in the zeroth order approximation. With $a_n^o = \beta$, C can be approximated by its convergence[25]

$$C \simeq (S/2)[1 + (1+4/S^2)^{1/2}] \tag{39}$$

$$C' \simeq (S'/2)[1 + (1 + 4/S'^2)^{1/2}] \tag{40}$$

where $S = 4\sigma\beta[2/(\beta^2 + \sigma^2)]^{1/2}/(1+\beta)$ and $S' = 4\sigma\beta^3[2/(\beta^2+\sigma^2)]^{3/2}/(1+\beta)$

With Eqs. (39) and (40), it is simple algebra to find from Eqs. (31) and (33) that

$$a_o = \beta\,[(C/C') - 1]^{1/2} \tag{41}$$

$$I_o = (\tilde{P}_o/C)(1+\beta^2/a_o^2)^{1/2} \tag{42}$$

$$a_1 = \beta\,[C'(C-\sigma_o)/C(C'-\sigma_o') - 1]^{1/2} \tag{43}$$

$$I_1 = (\tilde{P}_o/C)(1+\beta^2/a_1^2)^{1/2}\,(C-\sigma_o) \tag{44}$$

and so on for a_2, $a_3 \ldots$, I_2, $I_3 \ldots$. Expressions for a_n and I_n gets longer and messier as n becomes large. Here we will only quote the approximate expressions for extreme cases, although it is straight forward to get general results.

When $\beta \ll 1$, the saturated spectrum will exhibit many narrow lines. For simplicity of expression, we neglect terms of order β^2 compared to unity, thus

$$a_{2n} \simeq \beta \left\{ C'(1 - C \sum_{m=1}^{n} \sigma_{2m-1})/C(1 - C' \sum_{m=1}^{n} \sigma'_{2m-1}) - 1 \right\}^{1/2} \tag{45}$$

$$a_{2n+1} \simeq \beta \left\{ C'(C - \sum_{m=0}^{n} \sigma_{2m})/C(C' - \sum_{m=0}^{n} \sigma'_{2m}) - 1 \right\}^{1/2} \tag{46}$$

$$I_{2n} = (\tilde{P}_o/C)(1 - C \sum_{m=1}^{n} \sigma_{2m-1})(1 + \beta^2/a_{2n}^2)^{1/2} \tag{47}$$

$$I_{2n+1} = (\tilde{P}_o/C)(C - \sum_{m=0}^{n} \sigma_{2m})(1 + \beta^2/a_{2n+1}^2)^{1/2} \tag{48}$$

for $\beta \ll 1$. Since $\sigma'_n < \sigma_n$, Eqs. (45) - (48) shows that $a_n > a_{n-1}$ and $I_n < I_{n-1}$, i.e., the spectral lines will broaden and their intensity decreases as more cascade processes occur. The behavior of I_n agrees with previous theories on cascade mode coupling[10, 11] which approximated $a_n = 0$. Similar features of the saturated Langmuir wave spectrum are obtained in numerical calculations involving just ion nonlinear Landau damping.[8]

When $\beta \simeq 1$, if we neglect the nonlinear four-wave coupling process by setting $\sigma_n = \sigma'_n = 0$ in Eqs. (31) - (34), a spectrum with several distinct peaks are obtained in agreement with previous theories. However, when nonlinear four-wave coupling is included, it is found that a_n^2 quickly becomes

negative for $n \geq 1$. Thus, only a few lines will appear even if P_o is large. Especially, when $\beta \gtrsim 0.4$, the spectrum will show only one peak, with width and height

$$a_o = (\beta^2 - \sigma^2)^{1/2} \tag{49}$$

$$I_o = (\tilde{P}_o/\sigma_o)(1 + \beta^2/a_o^2)^{1/2} \tag{50}$$

Equations (45), (46) and (49) shows $a_n < \beta \simeq 1$, so that the approximation of including interaction between lines separated by Δ is justified.

For further iteration, we substitute Eqs. (41) - (44) etc., into Eq. (37), and carry out the above outlined procedure again. This is more easily done with numbers than with symbols. The following results are obtained by iterating seven times. Usually, the first-order results quoted in Eqs.(41 - (50) are within a factor of 2 of the final results, for both the $\beta \simeq 1$ and $\beta \ll 1$ cases.

Figures 4 - 6 show the saturated Langmuir wave spectra for a hydrogen plasma, with $\omega_o = 1.05\ \omega_{pe}$, $\gamma_\ell/\omega_{pe} = 10^{-3}$. The ion acoustic wave damping rate varies from $\beta = 0.05$ in Fig. 4 to $\beta = 0.5$ in Fig. 6. The qualitative difference between these spectra should be obvious. When $P_o/P_{th} = 5$, Fig. 6 which corresponds to the case $T_e \simeq T_i$ exhibits a single broad peak with width $\sim \Delta/2$ centering around the wavevector satisfied by linear decay resonance condition. With the same parameters but for the $T_e >> T_i$ case, Fig. 4 exhibits seven peaks with widths of the order $0.02\ \Delta$. While wave energy is spread to very long wavelength mode

via second decay processes in $\beta << 1$ cases (Figs. 4 and 5), such spread is absent in the $\beta \simeq 1$ case. The spectrum in Fig. 6 can be interpreted in terms of nonlinear four-wave coupling, which couples energy to waves with both lower and higher wavevector, but always close to the original linearly excited wavevector, in contrast to the cascade processes which spread energy to modes with smaller wavevector only. Note that in Fig. 6 $|E_o|^2/4\pi nT_e = 2 \times 10^{-3}$ for $P_o/P_{th} = 5$, and the wave energy concentrates in modes with wavevector $\lambda_o k \gtrsim 0.15$ so that $|E_o|^2/4\pi nT_e << (\lambda_D k)^2$ and strong nonlinear processes as Langmuir wave collapse will not occur.

V. TOTAL SATURATED WAVE ENERGY

The total saturated wave energy I_T is important because it determines the anomalous absorption rate. It is obtained by integrating the spectrum over all k. The spectrum is represented by the positive part of Eq. (26),

$$P_\ell = \int I(k)\, dk = \sum_n I_n \int_{k_{n-}}^{k_{n+}} \exp\left[-(k-k_n)^2/a_n^2\Delta^2\right] dk \tag{51}$$

where $k_{n\pm} = k_n \pm a_n\Delta\left[\ell n(I_n/P_{th})\right]^{1/2}$ defines the range of k-space excited by linear as well as nonlinear instabilities. Thus

$$P_\ell = \sqrt{\pi}\Delta \sum_{n=0}^{N} a_n I_n \operatorname{erfc}\left[\ell n\,(I_n/P_{th})\right]^{1/2} \tag{52}$$

which is approximately $P_\ell \simeq \sqrt{\pi}\Delta \sum_n a_n I_n$ when $P_o/P_{th} \gtrsim 3$. The number of modes N present in the spectrum is determined by the largest number such that $I_N \gtrsim \Gamma$. When $\beta << 1$, $P_o/P_{th} >> 1$, Eqs. (45) - (48) gives

$$N \simeq (2/S)\left\{1 + (\beta/\eta)^2\left[1 - (1 + 2\eta^2/\beta^2)\right]^{1/2}\right\} \tag{53}$$

where $\eta \equiv P_o/P_{th}$. Equation (53) shows that for any σ, β, N approaches a constant when $\eta >> 1$. Thus the total Langmuir wave energy Eq. (52) is directly proportional to P_o when $P_o >> P_{th}$. The $P_\ell \propto P_o$ dependence is observed experimentally.[13-15]

Below threshold, $P_o < P_{th}$, $P_\ell = 0$ since the present theory does not take into account thermal fluctuations. Close to threshold, $P_o \gtrsim P_{th}$, Eq. (52) shows the total Langmuir wave energy increases very rapidly as P_o, which is characteristic of parametric processes overcoming the threshold and agrees with experimental observations.[14, 15] Just how P_ℓ rises from zero to a level comparable to the pump when P_o increase by less than a factor of 2 depends on the detail shape of the spectrum. Since we have approximated the spectrum to be consisting of Gaussian lines in Eq.(26), the error-function dependence in Eq. (52) can only be a qualitative description.

Figure 7 plots the total Langmuir wave energy in a hydrogen plasma excited by parametric instability. The three curves in Fig. 7 correspond to integrating over the spectra depicted in Figs. 4 - 6 respectively. It can be seen that saturated wave energy is of the order of the pump energy, in agreement with experiments[12-15] as well as simulations.[4, 5] Also, a higher damping rate for the acoustic wave gives a lower saturated wave energy, which is physically reasonable because higher damping means energy is being transferred faster to the particles. Note that the maximum pumping level in Fig. 7 is for the $\beta = 0.5$, $P_o/P_{th} = 10$ case, where $|E_o|^2/4\pi nT_e \simeq 0.02$ and the corresponding linear growth rate $\sim 0.7\ \omega_a$, so that the present weak turbulence calculation is applicable.

VI. DISCUSSION

In summary, we have studied the saturation of parametric decay instability by nonlinear three- and four-wave coupling as well as ion nonlinear Landau damping. The relative importance of these saturating mechanisms is determined by the damping rate of the ion acoustic wave γ_a/ω_i, which is treated as a varying parameter. A steady-state solution to the solution is developed during which various approximations have been made. Here we investigate the stability of our steady-state solution, and briefly discuss the effect and range of validity of the major approximations involved.

Keeping the time variable, Eq. (25) becomes

$$(\partial/\partial\tau + P_{th} - f_d P_o)I(k)$$
$$= -(1+\beta)I(k)\int I(k')dk'\left\{f[(k'-k+\Delta)/\beta\Delta] - f[(k'-k-\Delta)/\beta\Delta] + 4\beta' f[(k-k')/\sigma\Delta]\right\} \tag{54}$$

where $\tau \equiv (\omega_a\omega_\ell/\gamma_a)t$ and $\beta' = \beta/(1+\beta)$. We let $I(k) = I_o(k) + \delta I(k)$ where $I_o(k)$ is the steady-state solution of Eq. (26) and $\delta I(k)$ is a small time dependent perturbation term. If $\delta I(k)$ decays exponentially in time, then the steady-state solution $I_o(k)$ is stable. Linearize the right-hand side of Eq. (54) with respect to $\delta I(k)$, and approximate the f's by delta functions when integrating the $\delta I(k)$ term, we get

$$\partial\delta I(k)/\partial\tau + \left\{-f_d P_o + (1+\beta)I_o(k)\,[4\beta' + G(k)]\right\}\delta I(k) + (1+\beta)\,I_o(k)\left\{\delta I(k-\Delta) - \delta I(k+\Delta)\right\} = (\tag{55}$$

where $G(k)$ is given by the right-hand side of Eq. (28). Consistant with the approximations made in Sec. IV, we can assume interaction between modes separated by $\pm\Delta$ only, then Eq. (55) breaks up to a set of N coupled equations. The stability condition involves finding the eigenvalue of an N x N matrix.

When $\beta \ll 1$, nonlinear four-wave coupling is negligible compared to cascade mode coupling, so that although the physical condition and saturating mechansim is different, mathematically the problem is equivalent to the ion nonlinear Landau damping theory. The time evolution of Langmuir waves has been calculated numerically in Ref. 8, which reported steady-state wave spectra very similar to the present result, i.e., a spiky spectrum consisting of many distinct lines. Thus it is assumed here that our steady-state solution is stable. Moreover, a spiky spectrum as predicted is actually observed in experiment[16, 17] with appropriate physical condition ($T_e \gg T_i$ corresponding to $\beta \ll 1$), thus providing the best justification for the stability of the present steady-state solution.

In the $\beta \simeq 1$ case, the steady-state spectrum consists of a single peak and Eq. (55) becomes

$$\partial \delta I(k)/\partial \tau + \left\{ 4\beta'(1+\beta) I_o(k) \left[1 + a_o \sqrt{\pi}\ \Delta\sigma I_o (a_o^2 + \sigma^2)^{-1/2} \right] - P_o \right\} \delta I(k) = 0 \tag{56}$$

$\delta I(k)$ will decay exponentially with time if the quantity in the curly bracket is positive. When $\sigma \ll 1$, this condition is satisfied if

$$(\sigma \Delta P_o + 1/4)^{1/2} - 1/2 < \beta < 4\sqrt{\pi} - 1. \tag{57}$$

Since $\sigma, \Delta\ P_o \ll 1$, the stability condition Eq. (57) shows that the steady-state solution is stable for a wide range of $\beta < 1$.

When $\beta > 1.25$, our solution becomes unstable. Actually, since the coupling width of three-wave processes is proportional to $\beta\Delta$, by retaining coupling between modes separated by Δ we have already limited ourselves to the case $\beta < 1$. Thus the present theory is valid only for $\beta < 1$.

In this theory, the exact plasma dispersion relation is approximated by a Gaussian function in wavenumber. This approximation restricts the problem to one dimension. Following this approximation, we have assumed a solution consisting of Gaussian lines. By itself, the Gaussian approximation is reasonable, but since the integral equation we attempt to solve is sensitive to the tail of the coupling function, this approximation may have a subtle effect on the plasma wave spectrum. However, its effects on the total Langmuir wave energy should be small because of the integration over the entire spectrum.

Also, the calculation of the saturated spectrum is carried out in the random phase approximation so that wave energy is not spread very far into the high wavenumber region. To investigate energy spread into very low phase velocity modes, a coherent phase calculation has to be carried out.

ACKNOWLEDGEMENT

The author would like to thank Professor M. Porkolab for helpful discussions.

REFERENCES

* Supported by the National Science Foundation.

1. See, e.g., the review by M. Porkolab, Physica 82C, 86 (1976).

2. W.L. Kruer, P.K. Kaw, J.M. Dawson and C. Oberman, Phys. Rev. Lett. 24, 987 (1970).

3. See e.g., the review by W.L. Kruer, in Advances in Plasma Physics, A. Simon and W.B. Thompson, Eds., (Academic, New York, 1971), Vol. 6, p. 237.

4. W.L. Kruer and J.M. Dawson, Phys. Fluids 15, 446 (1972).

5. J.S. DeGroot and J.J. Katz, Phys. Fluids 16, 401 (1973).

6. J.J. Thomson, R.J. Faehl, and W. L. Kruer, Phys. Rev. Lett. 31, 918 (1973); J.J. Thomson, R.J. Faehl, W.L. Kruer and S. Bodner, Phys. Fluids 17, 973 (1974).

7. G.J. Morales, Y.C. Lee and R.B. White, Phys. Rev. Lett. 32, 157 (1974).

8. E.J. Valeo, C. Oberman and F.W. Perkins, Phys. Rev. Lett. 28, 340 (1972); W.L. Kruer and E.J. Valeo, Phys. Fluids 16, 675 (1973).

9. D.F. Dubois and M.V. Goldman, Phys. Rev. Lett. 28, 218 (1972); Phys. Fluids 15, 919 (1972).

10. Y.Y. Kuo and J.A. Fejer, Phys. Rev. Lett. 29, 1667 (1972).

11. S.Y. Yuen, Phys. Fluids 18, 1308 (1975).

12. T.K. Chu and H. Hendel, Phys. Rev. Lett. 29, 634 (1972).

13. K. Mizuno and J.S. DeGroot, Phys. Rev. Lett. 35, 219 (1975).

14. J. T. Flick, Ph.D. Thesis, Department of Astrophysical Sciences, Princeton University, 1975.

15. J.T. Flick and H. Hendel, Princeton Plasma Physics Laboratory Report MATT-1106, 1975.

16. R. Stenzel and A. Wong, Phys. Rev. Lett. 28, 274 (1972).

17. M. Mizuno and J.S.DeGroot, private communication.

18. S.Y. Yuen, Phys.Rev. Lett. 40, 269 (1978).

19. K. Nishikawa, J. Phys. Soc. Jpn. 24, 916 (1968).

20. V.E. Zakharov, Soviet Physics JETP 35, 908 (1972).

21. S.Y. Yuen, Phys. Lett. A53, 185 (1975).

22. R.Z.Sagdeev and A.A. Galeev, Nonlinear Plasma Theory (W.A. Benjamin, Inc., N.Y., 1969) Chap. III.

23. D.F. Dubois and M.V. Goldman, Phys. Rev. 164, 207 (1967).

24. B.D. Fried and S.D. Conte, The Plasma Dispersion Function, (Academic Press, N.Y., 1961.

25. H.S. Wall, Analytic Theory of Continued Fractions (D.van Nostrand, N.Y., 1948) Chap. 1.

FIGURE CAPTIONS

1. Coupling processes considered in this paper: a) parametric decay instability, b) OTSI, c) three-wave decay coupling, d) three-wave coalescence, e) nonlinear coupling of four Langmuir waves f) ion nonlinear Landau damping.

2. Matrix element for nonlinear ion Landau damping. The solid line plots $M(\zeta)$ for $T_e = T_i$. Dashed line and the crosses plots $0.6\left\{f[(k-k'-\Delta)/\beta\Delta] - f[(k-k'+\Delta)\beta\Delta]\right\}$ for $\beta = \sqrt{3}$, the dashed line with $f(x) = (1+x^2)^{-1}$, crosses with $f(x) = \exp(-x^2)$ for any x.

3. Linear growth rate as a function of normalized wavevector for hydrogen plasma. $\epsilon = 0.05$, $\gamma_\ell/\omega_{pe} = 3 \times 10^{-3}$, $\gamma_a/\omega_a = 0.3$, a) $P_o = 4 \times 10^{-3}$, b) $P_o = 0.01$, c) $P_o = 0.05$.

4. Steady state Langmuir wave spectrum for hydrogen plasma with $\omega_o = 1.05\ \omega_{pe}$, $\gamma_\ell/\omega_{pe} = 10^{-3}$, $\gamma_a/\omega_a = 0.05$, $P_o/P_{th} = 5$. The arrow marks the wavevector of the pump frequency if it satisfies the Bohm-Gross dispersion relation.

5. Steady state Langmuir wave spectrum. Same parameters as Fig. 4 except $\gamma_a/\omega_a = 0.1$.

6. Steady state Langmuir wave spectrum. Same parameters as Fig. 4 except $\gamma_a/\omega_a = 0.5$.

7. Total saturated Langmuir wave energy as a function of pump intensity, $\omega_o = 1.05\ \omega_{pe}$, $\gamma_\ell/\omega_{pe} = 10^{-3}$.

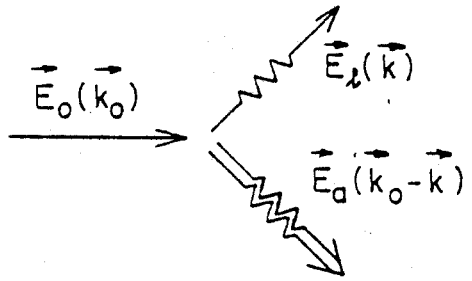

(a) $\omega_0 = \omega_{\ell\vec{k}} + \omega_{a\,\vec{k}_0-\vec{k}}$

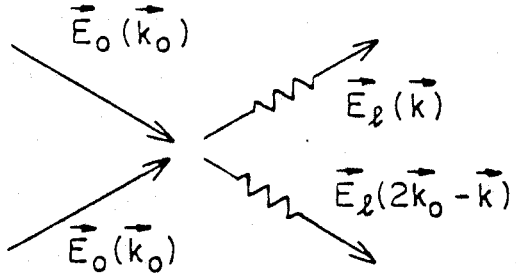

(b) $2\omega_0 = \omega_{\ell\vec{k}} + \omega_{\ell\,2\vec{k}_0-\vec{k}}$

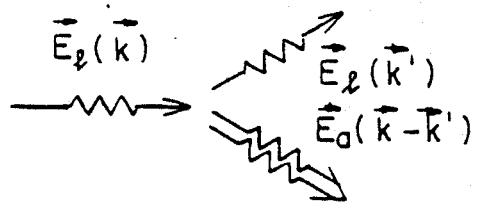

(c) $\omega_{\ell\vec{k}} = \omega_{\ell\vec{k}'} + \omega_{a\,\vec{k}-\vec{k}'}$

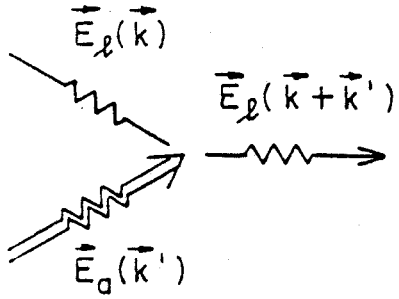

(d) $\omega_{\ell\vec{k}+\vec{k}'} = \omega_{\ell\vec{k}} + \omega_{a\vec{k}'}$

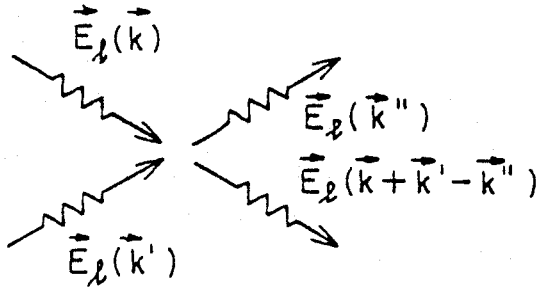

(e) $\omega_{\ell\vec{k}} + \omega_{\ell\vec{k}'} = \omega_{\ell\vec{k}''} + \omega_{\ell\vec{k}+\vec{k}'-\vec{k}''}$

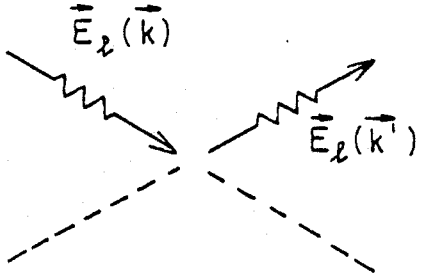

(f)

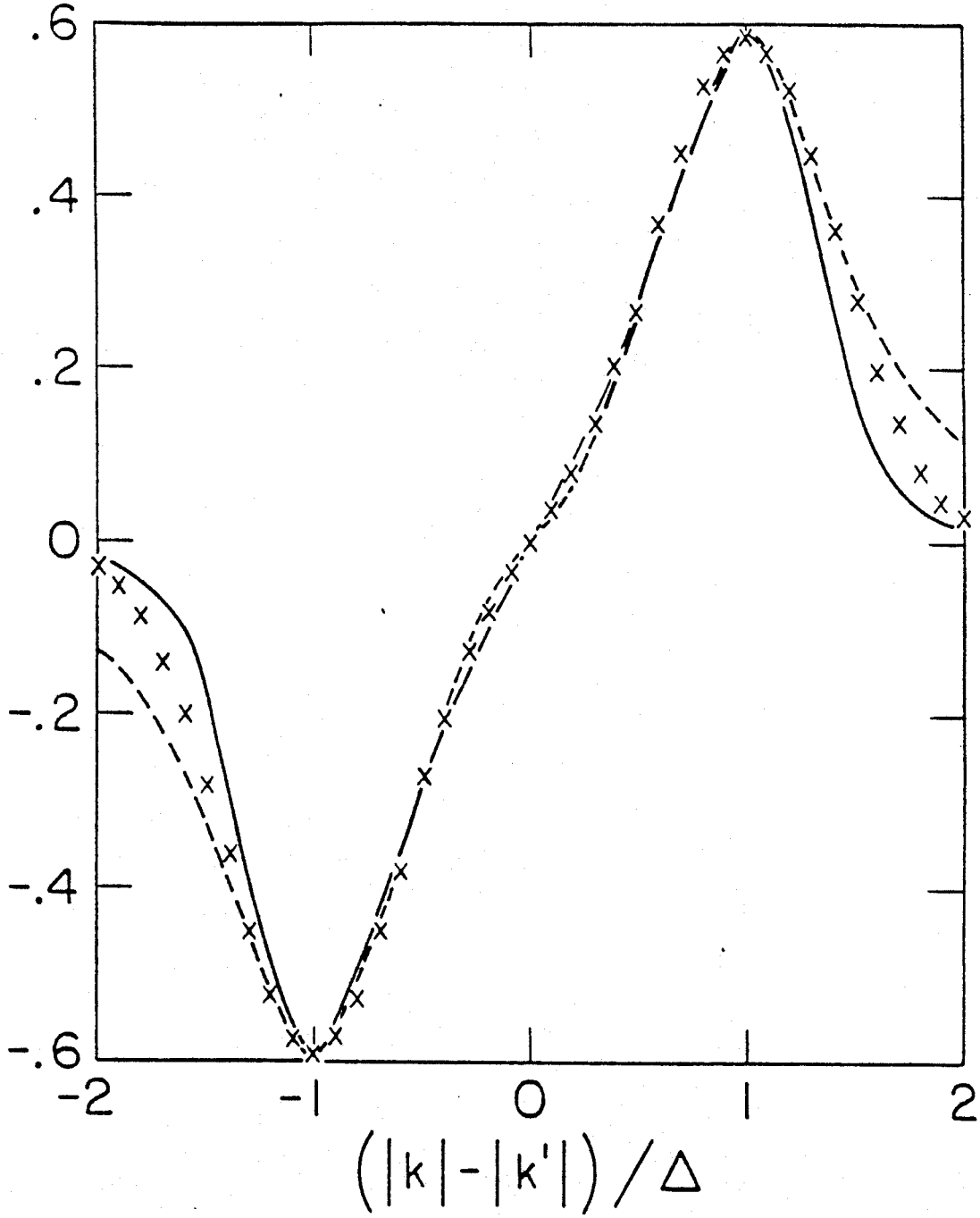
.6
.4
.2
0
-.2
-.4
-.6
-2
-1
0
1
2
(|k|-|k'|)/Δ

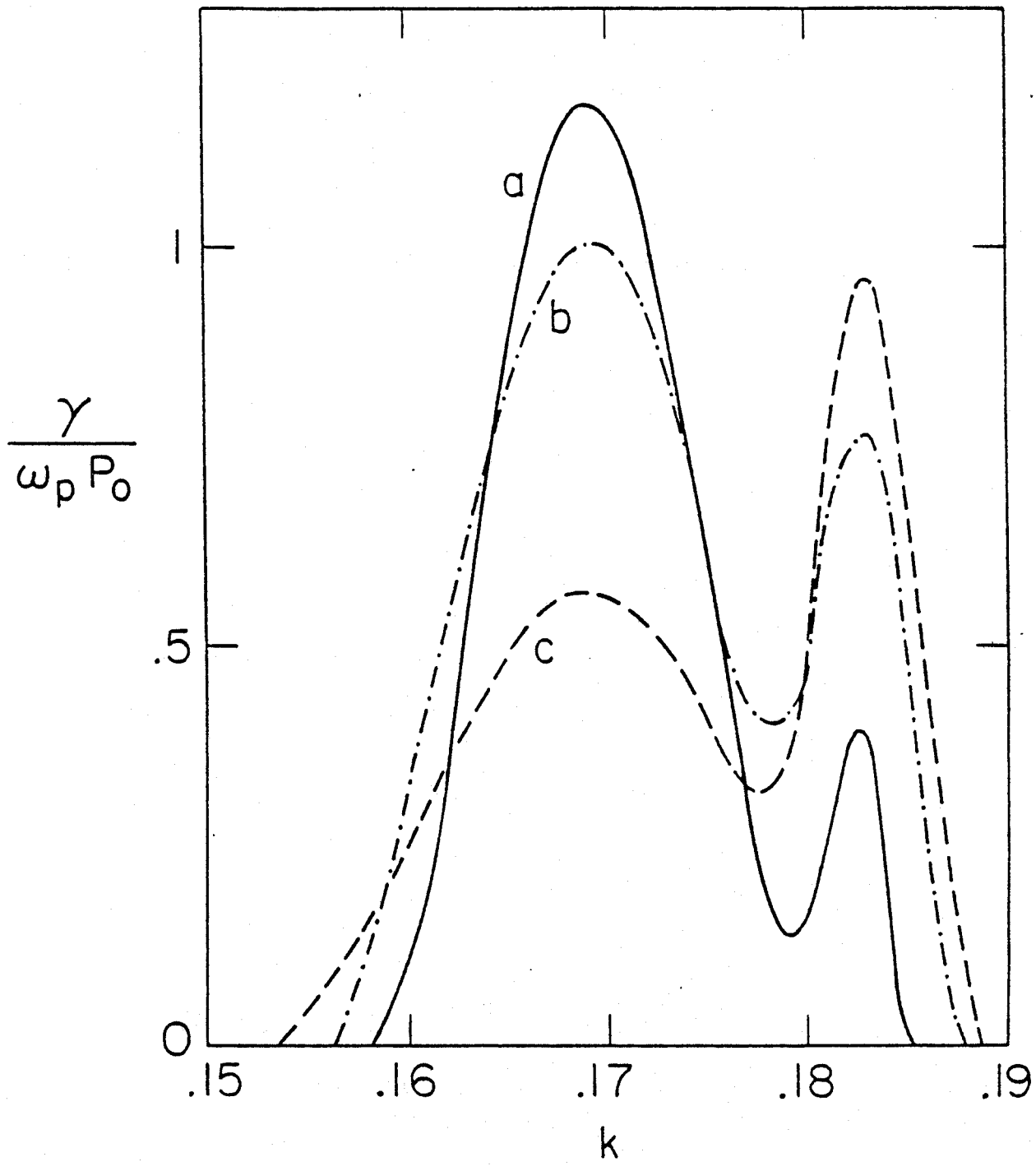
a
b
c
1
.5
0
.15
.16
.17
.18
.19
k
γ / ω_p P_o

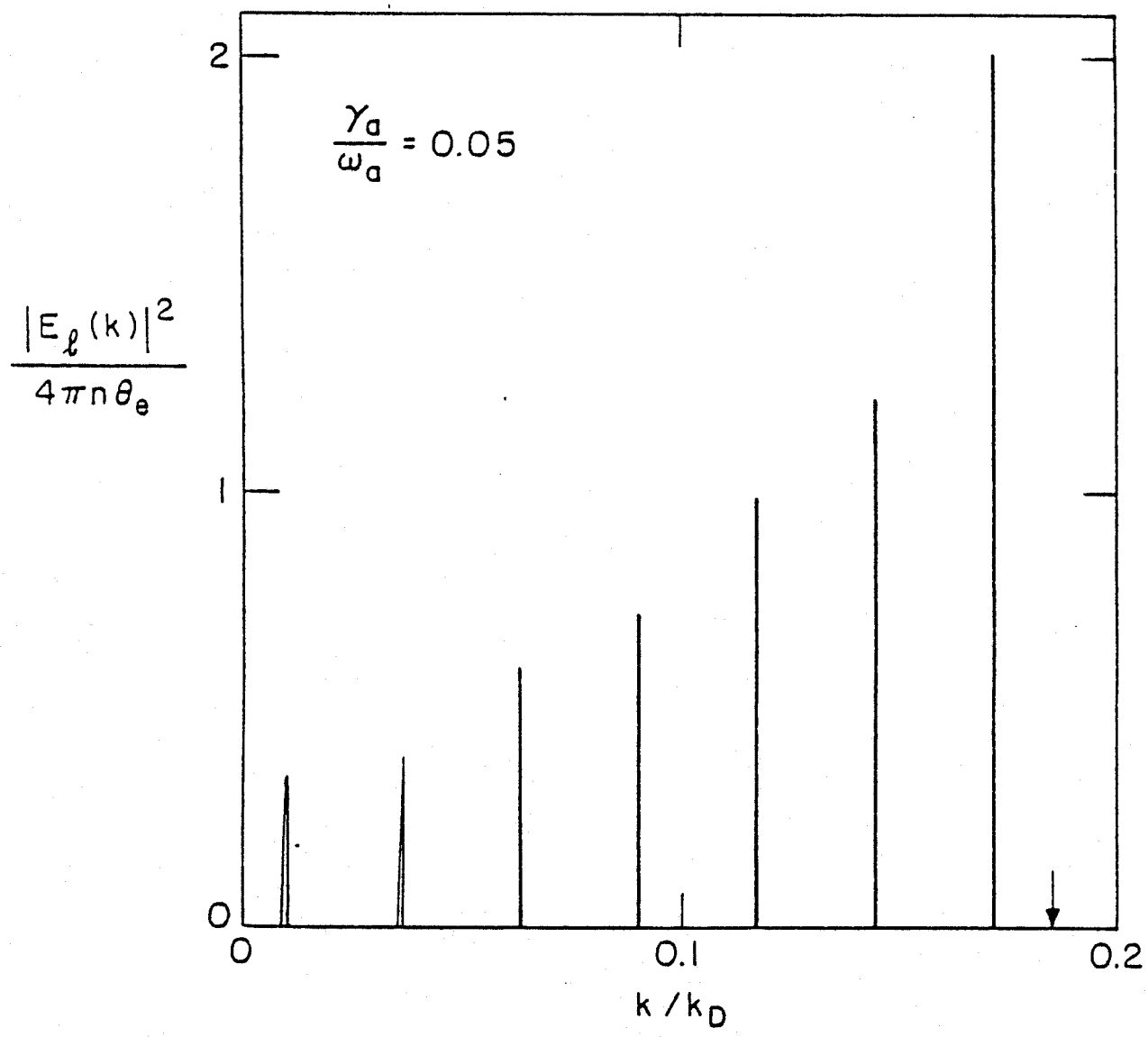
$\frac{|E_\ell(k)|^2}{4\pi n \theta_e}$
2
1
0
$\frac{\gamma_a}{\omega_a} = 0.05$
0
0.1
0.2
k/k_D

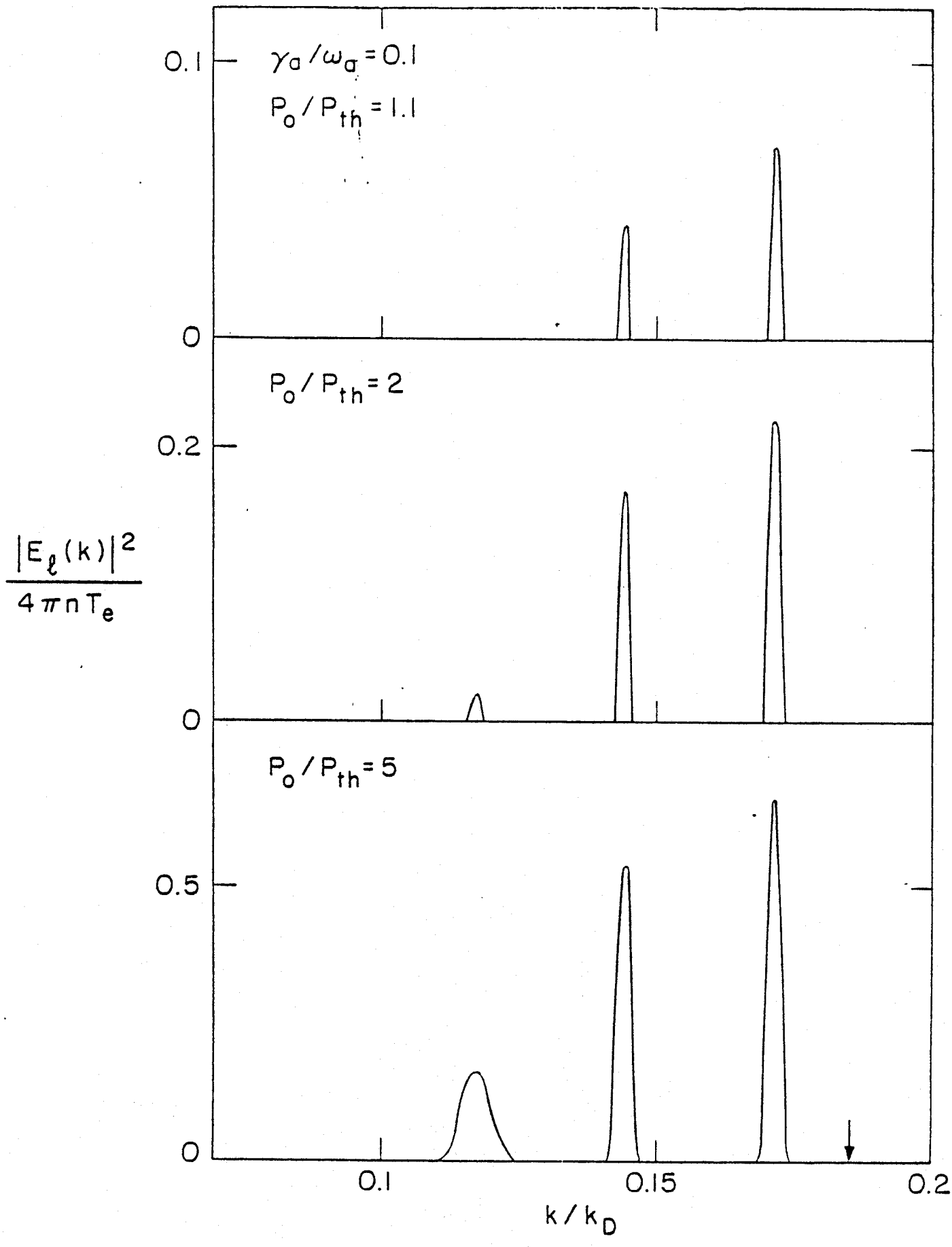
$\gamma_a/\omega_a = 0.1$
$P_o/P_{th} = 1.1$
$P_o/P_{th} = 2$
$P_o/P_{th} = 5$
0.1
0
0.2
0
0.5
0
0.1
0.15
0.2
k/k_D
$\frac{|E_\ell(k)|^2}{4\pi n T_e}$

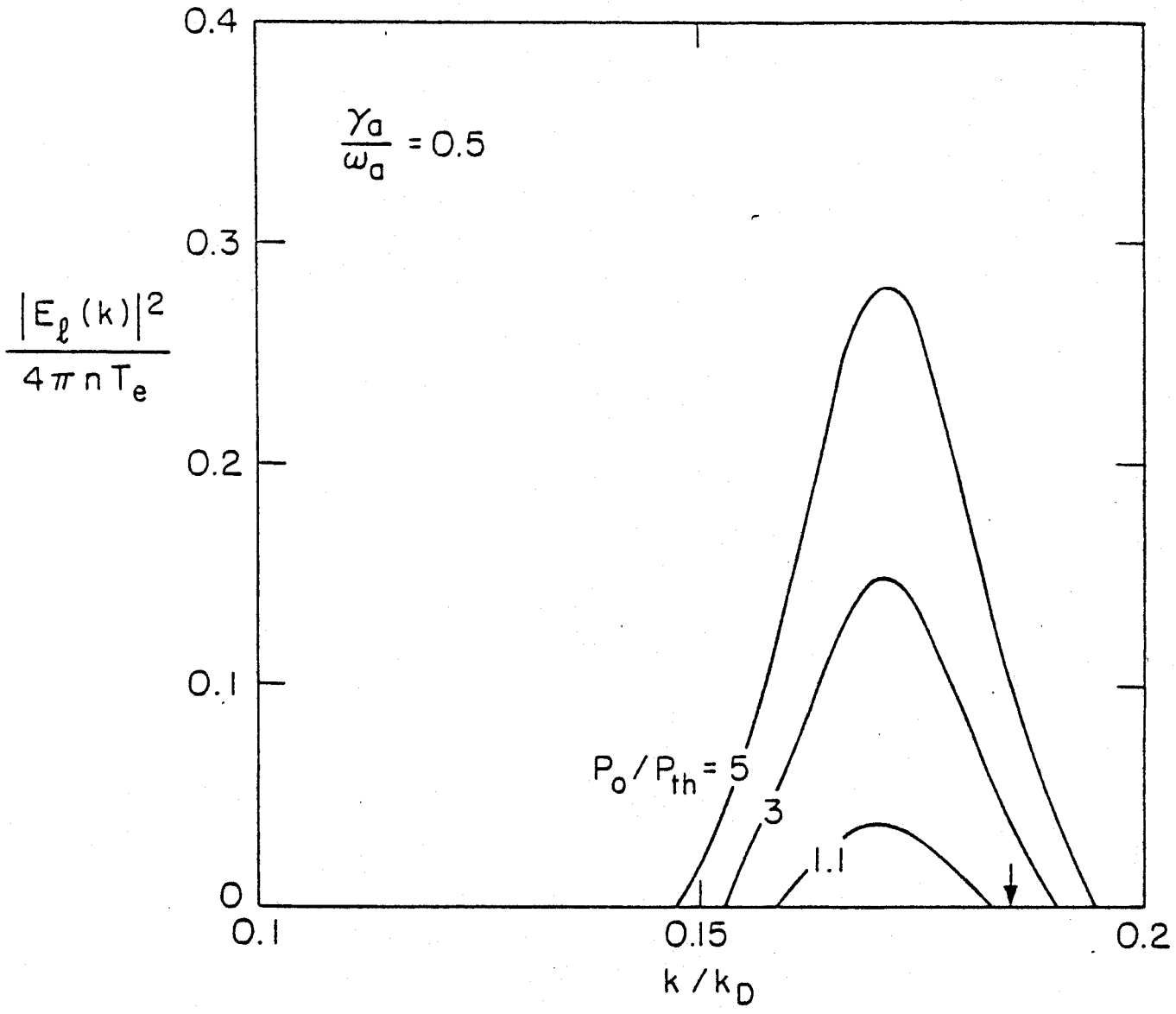
0.4
$\frac{\gamma_a}{\omega_a} = 0.5$
0.3
$\frac{|E_\ell(k)|^2}{4\pi n T_e}$
0.2
0.1
$P_o / P_{th} = 5$
3
1.1
0
0.1
0.15
0.2
k / k_D

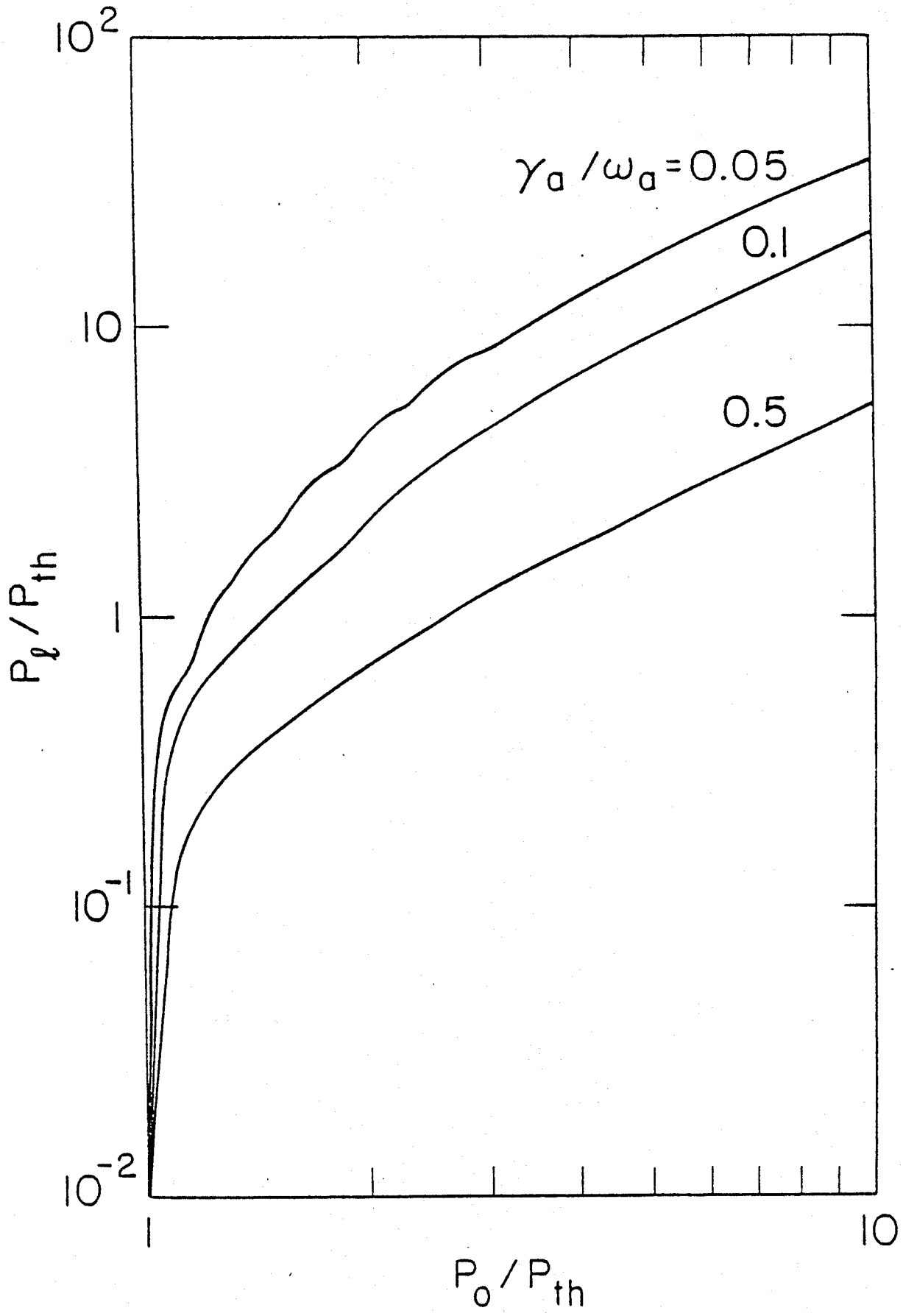
10^2
10
1
10^{-1}
10^{-2}
P_ℓ / P_{th}
$\gamma_a / \omega_a = 0.05$
0.1
0.5
1
10
P_0 / P_{th}

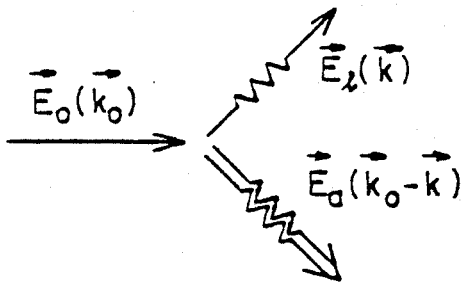

(a) $\omega_o = \omega_{\ell\vec{k}} + \omega_{a\,\vec{k}_o-\vec{k}}$

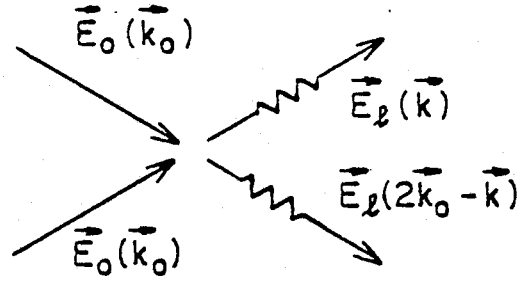

(b) $2\omega_o = \omega_{\ell\vec{k}} + \omega_{\ell\,2\vec{k}_o-\vec{k}}$

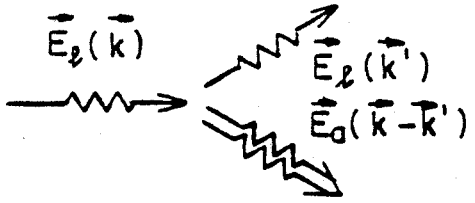

(c) $\omega_{\ell\vec{k}} = \omega_{\ell\vec{k}'} + \omega_{a\,\vec{k}-\vec{k}'}$

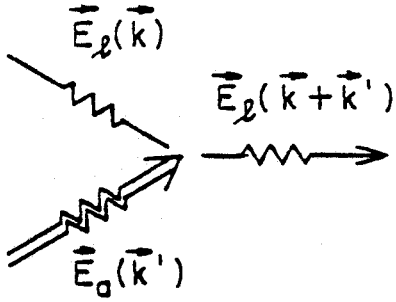

(d) $\omega_{\ell\vec{k}+\vec{k}'} = \omega_{\ell\vec{k}} + \omega_{a\vec{k}'}$

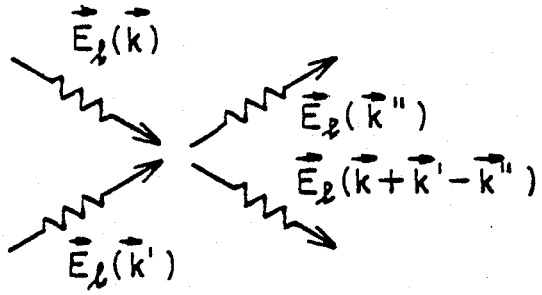

(e) $\omega_{\ell\vec{k}} + \omega_{\ell\vec{k}'} = \omega_{\ell\vec{k}''} + \omega_{\ell\vec{k}+\vec{k}'-\vec{k}''}$

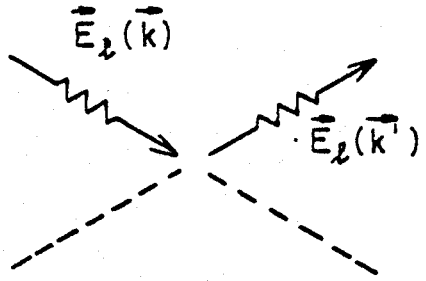

(f)

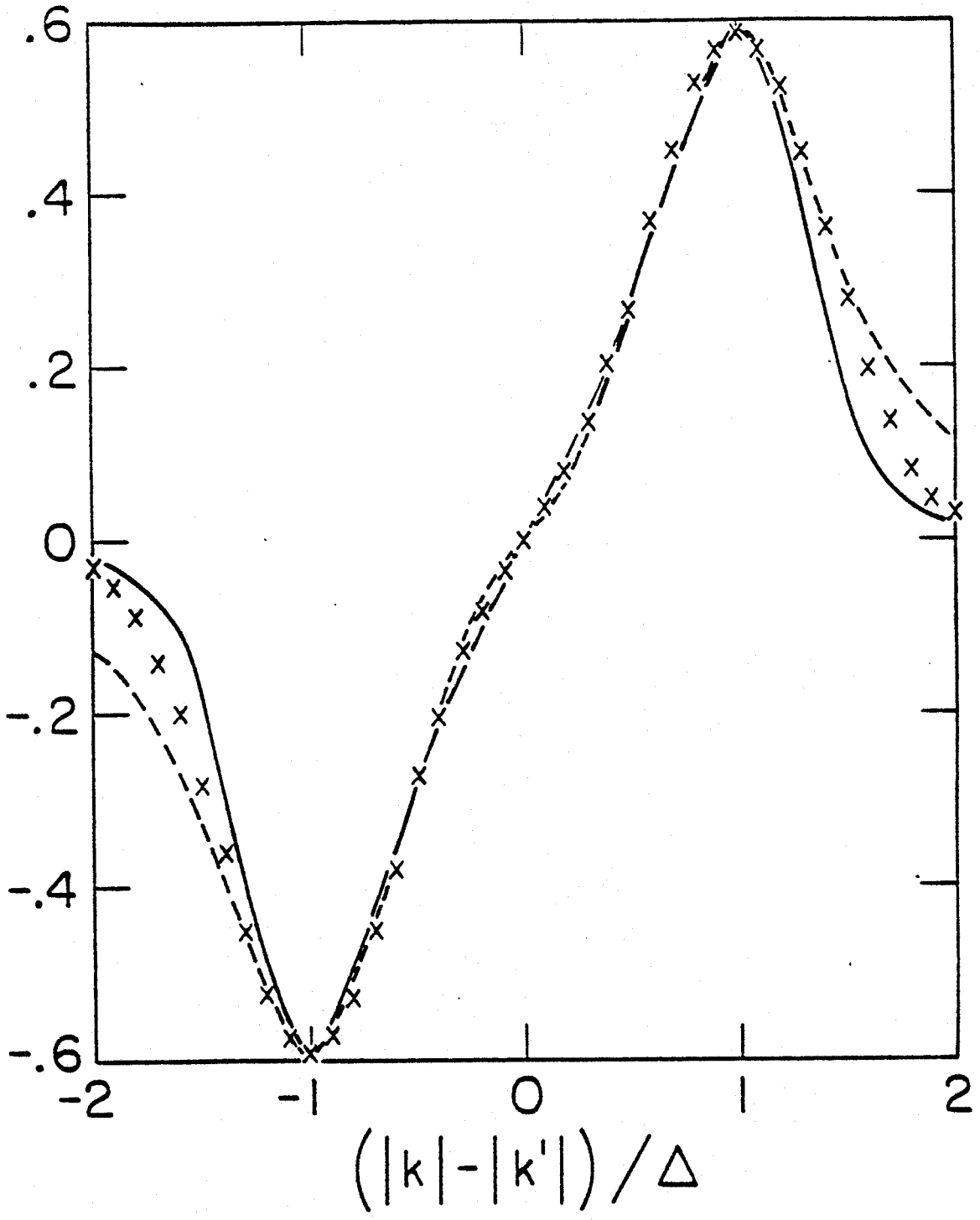
.6
.4
.2
0
-.2
-.4
-.6
-2
-1
0
1
2
(|k|-|k'|)/Δ

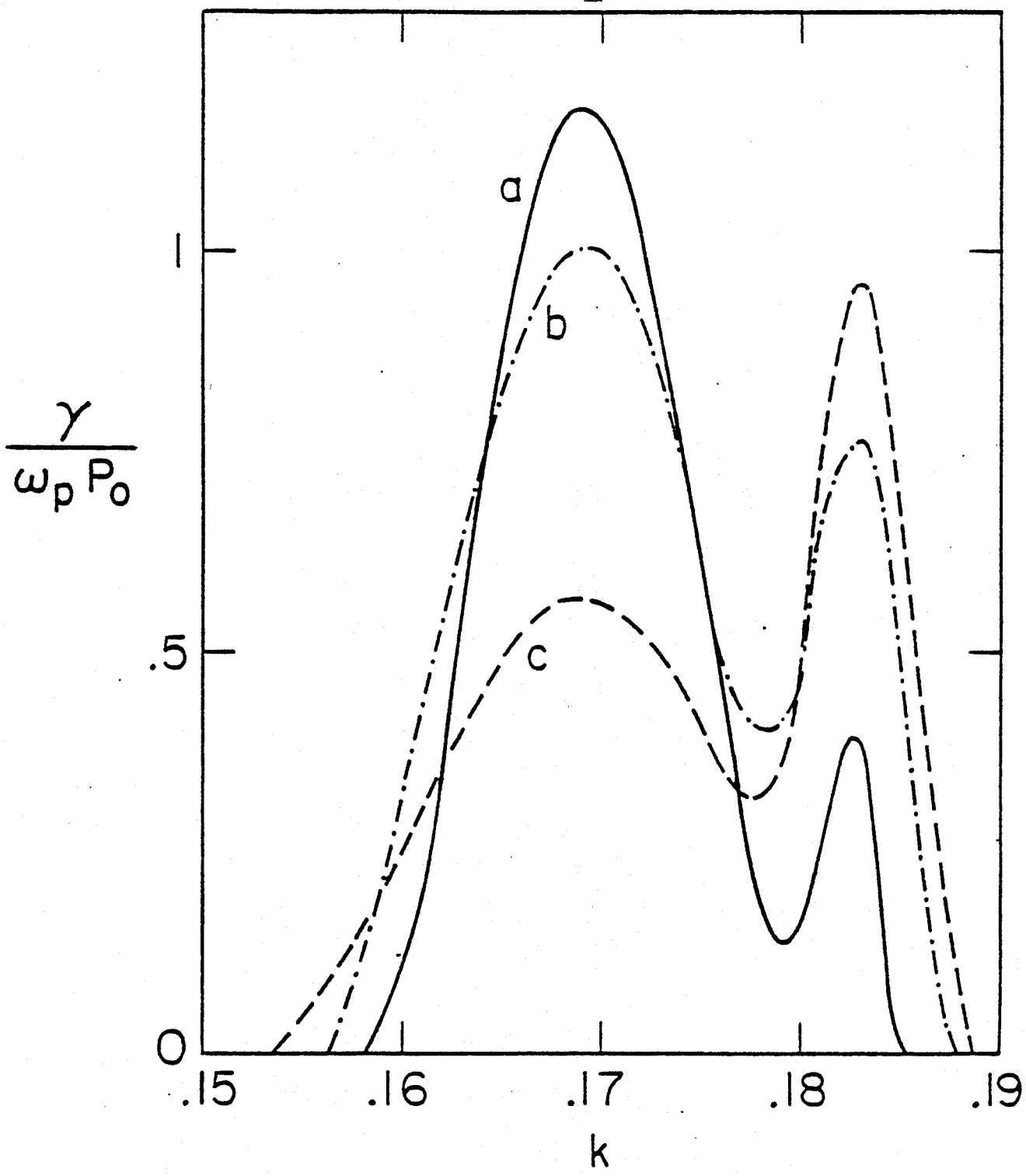
a
b
c
1
.5
0
.15
.16
.17
.18
.19
k
γ / ω_p P_o

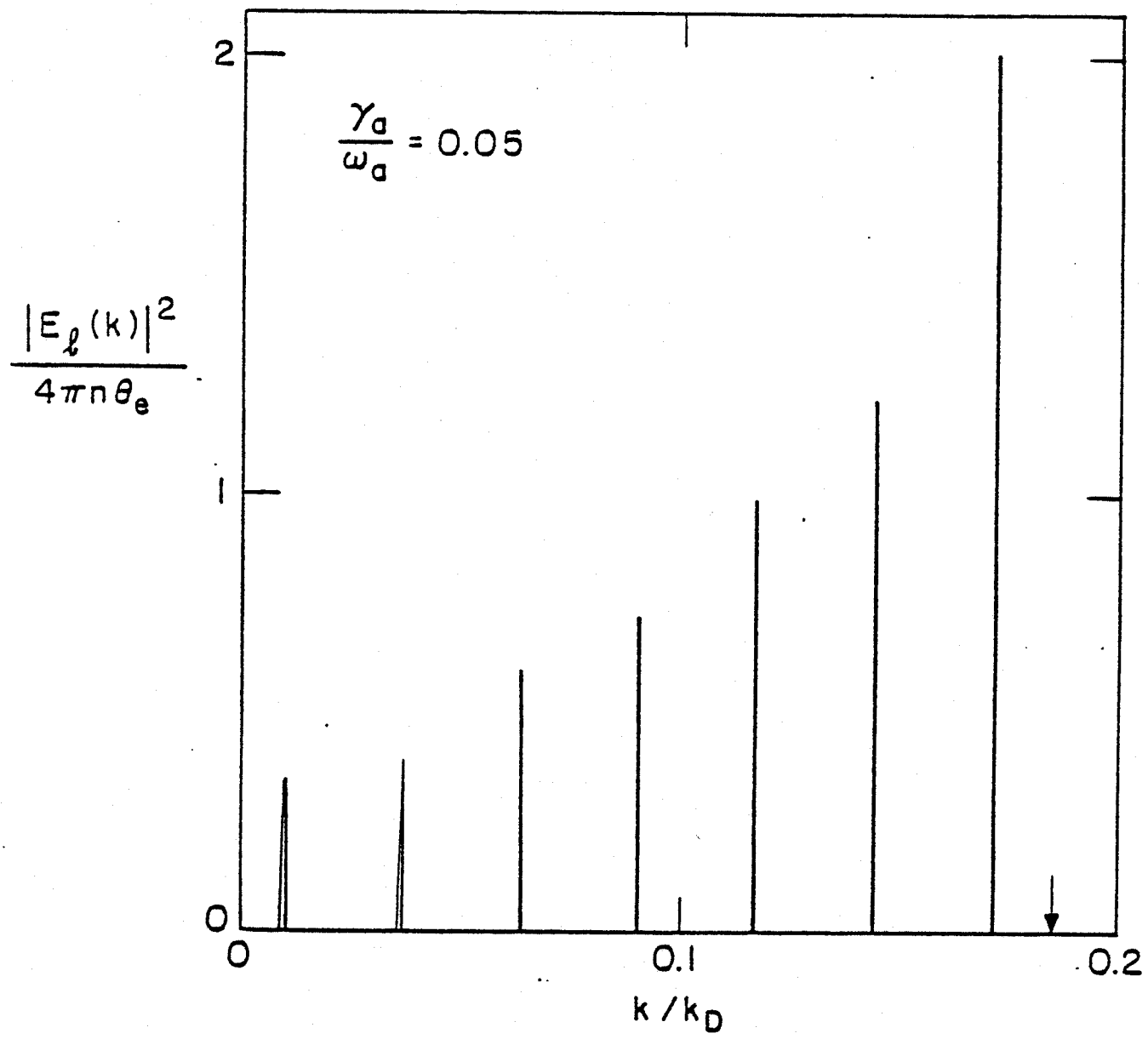
$\frac{\gamma_a}{\omega_a} = 0.05$
$\frac{|E_\ell(k)|^2}{4\pi n \theta_e}$
2
1
0
0
0.1
0.2
k/k_D

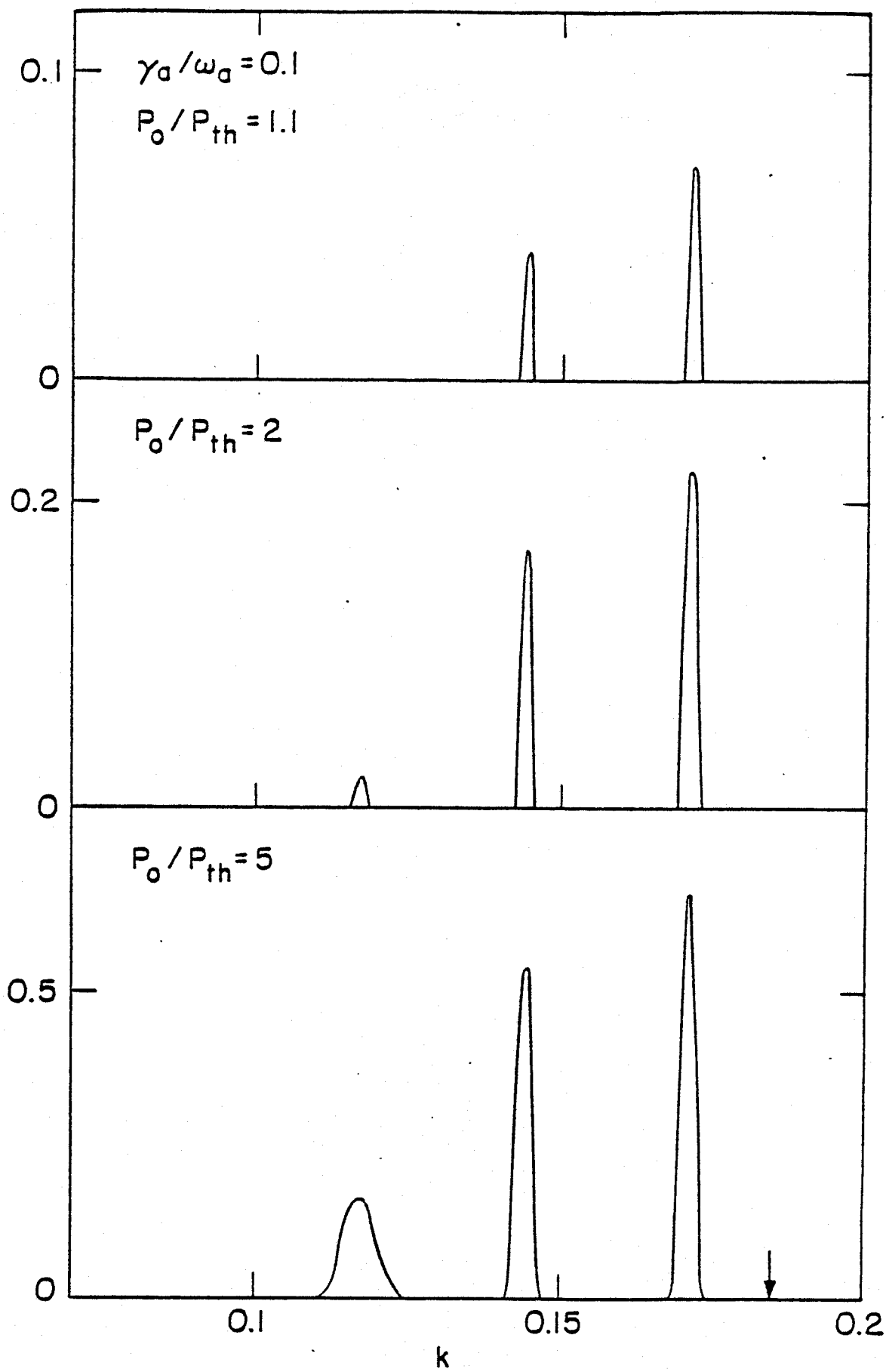

$\frac{|E_\ell(k)|^2}{4\pi n T_e}$

-3C
Fig 2

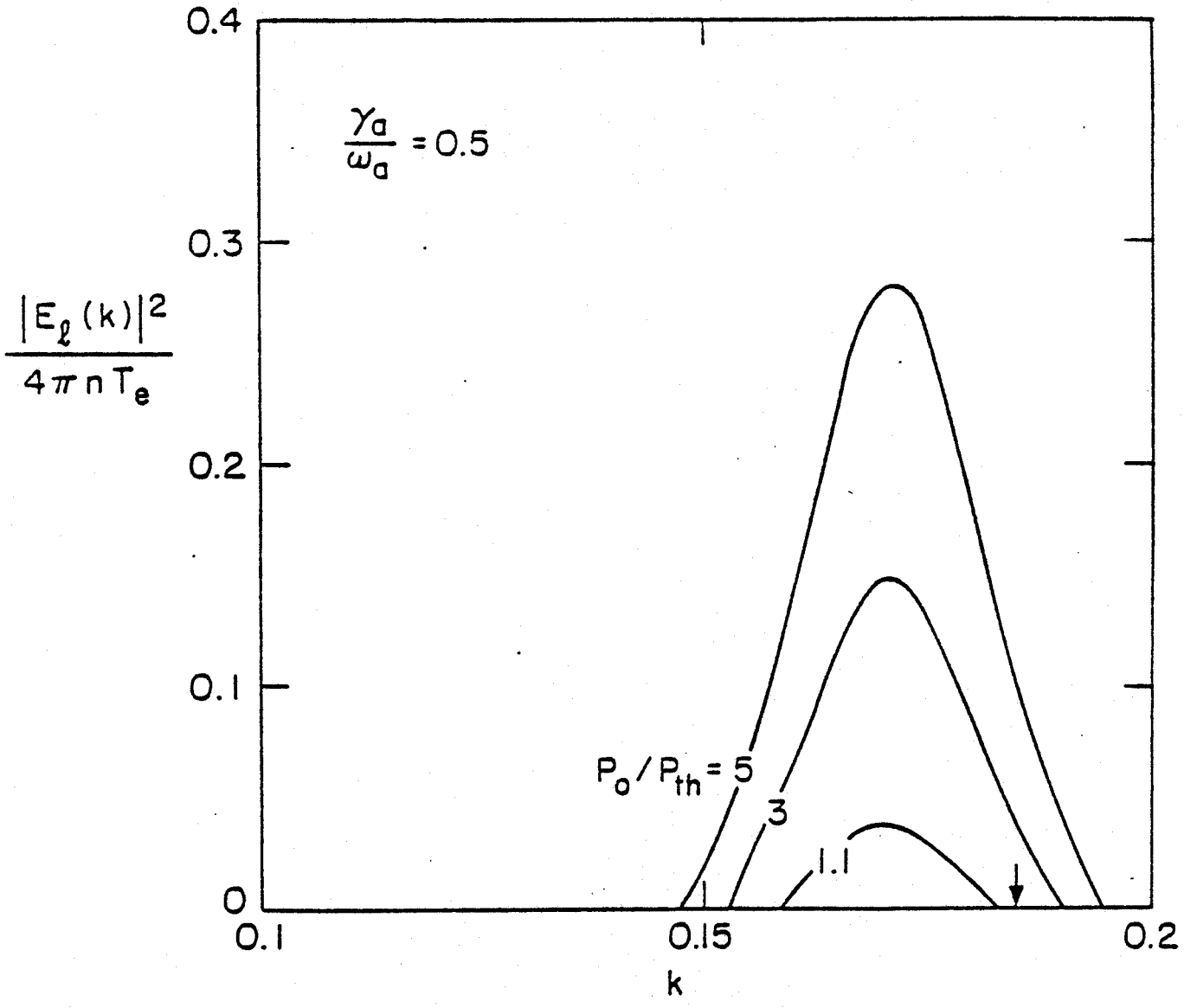
0.4
0.3
0.2
0.1
0
$\frac{|E_\ell(k)|^2}{4\pi n T_e}$
$\frac{\gamma_a}{\omega_a} = 0.5$
$P_o / P_{th} = 5$
3
1.1
0.1
0.15
0.2
k

Fig. 6

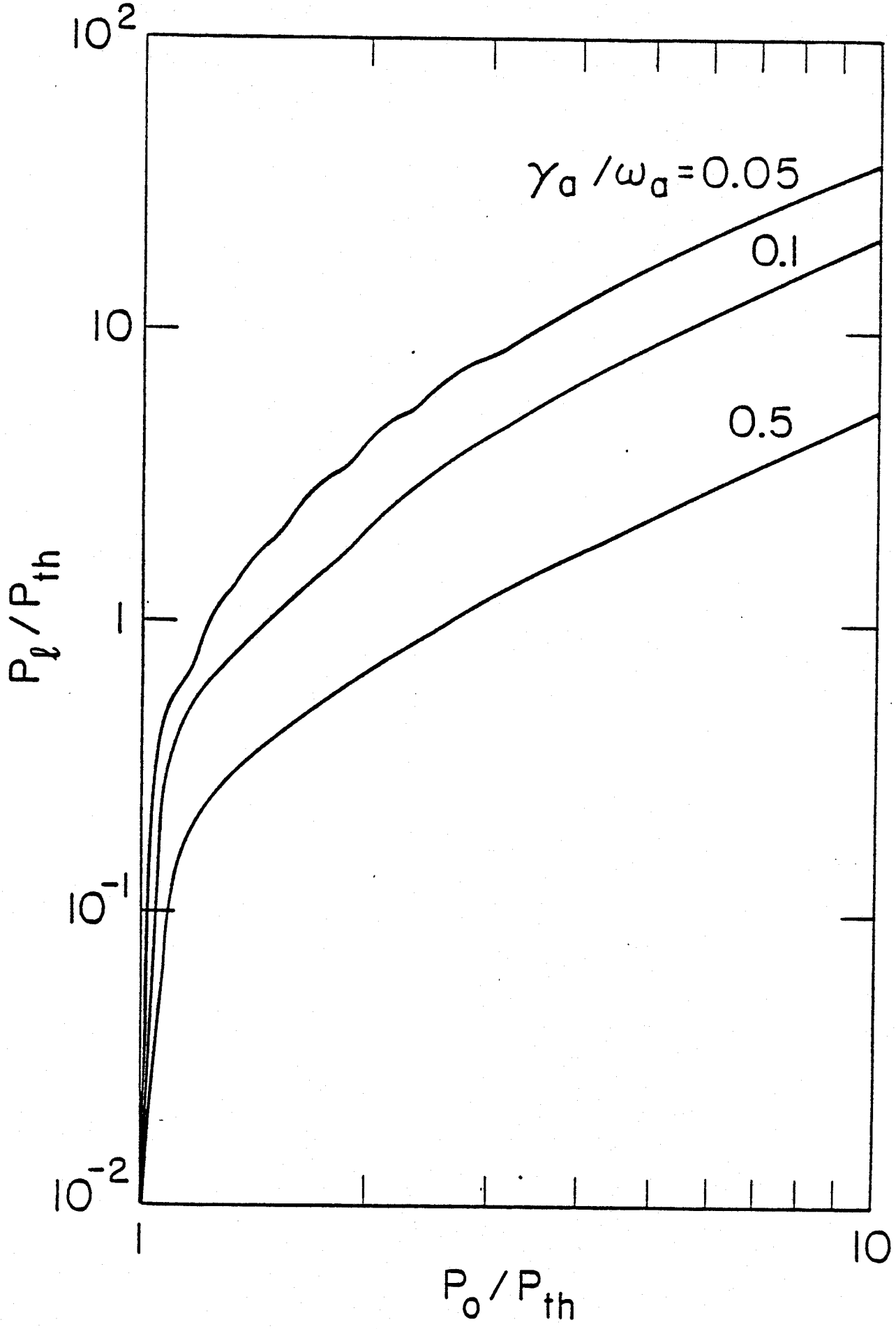
10^2
10
1
10^{-1}
10^{-2}
$\gamma_a / \omega_a = 0.05$
0.1
0.5
P_ℓ / P_{th}
1
10
P_0 / P_{th}